ASSESSMENT OF CLIMATE CHANGE IMPACT ON HYDROLOGICAL REGIME OF MAHANADI RIVER

A Dissertation

submitted in partial fulfilment of the requirement

for the award of degree of

Masters in Technology

In

Environmental Science and Technology

Submitted by

Ankit Kamboj

Roll. no. 601601003

under the guidance of

Dr. Richa Babbar
Assistant Professor
Department of civil Engineering
TIET

Dr. Vaibhav Garg
Scientist/Engineer – SE
Water Resource Department
IIRS / ISRO

SCHOOL OF ENERGY AND ENVIRONMENT

THAPAR INSTITUTE OF ENGINEERING AND TECHNOLOGY, PATIALA

(Declared as Deemed-to-be-University u/s 3 of the UGC Act, 1956)

JUNE 2018

DECLARATION CUM CERTIFICATE

I hereby declare that the project work entitled **"Assessment of Climate Change Impact on Hydrological Regime of Mahanadi River"** is an authentic record of my own work carried out at Indian Institute of Remote Sensing as requirements of one year project internship for the award of degree of M.Tech(Environmental Science and Technology), Thapar Institute of Engg. & Technology, Patiala, under the guidance of Dr. Vaibhav Garg and Dr. Richa Babbar, during June 15-2017 to June 15-2018

Ankit Kamboj

Ankit Kamboj

601601003

Date: 20 - 06 - 2018

Certified that the above statement made by the student is correct to the best of our knowledge and belief.

Dr. Richa Babbar
Assistant Professor
Civil Engineer Department

Dr. Vaibhav Garg
Scientist/Engineer-SE
Water resource Department

ACKNOWLDGEMENT

Learning is continuous process and to learn something you need purpose, motivation and guidance. Purpose comes from one's own impulse to learn and inquisitiveness, and to quench the quest of one's purpose one need motivation and guidance. In my quest of learning remote sensing and GIS, there were several around me who acted as lighthouse for me to navigate through the sea of hurdles.

I am very indebted to **Dr. Prakash Chauhan**, Director IIRS and **Dr. S.P Aggarwal**, Group Head of Water Resources Department for providing the support and infrastructure required at institution level for the implementation of this project.

By hearty, I would like to express my sincere gratitude to my supervisor **Dr. Vaibhav Garg** and **Dr. Richa Babbar** for their invaluable guidance, advice and support throughout the span of project. Cool, calm and cheerful nature of Vaibhav sir has always acted as safety valve and kept me out of pressure. Whole Water Resources Department had been a great source of encouragement. Their motivation and help have been a source of great inspiration to me.

I express my deep sense to **Dr. Bhaskar R.Nikam** for his guidance and support at IIRS Dehradun. It was always motivational to me while watching him working up late nights in his office. Whenever I meet to him he had long discussion and asked the status of my research work, from his busy schedule.

I heartily thank to Yogesh joshi, Sidarth Arora, Adrija Roy, Aswathi PV, Rajeev Ranjan, Vardan singh, Suvrat. I also thank all CMA member for technical help. List is long so thanks all the M.Tech batch of 2016-2018 batch (TIET) and Ravi, making my days in IIRS wonderful.

Last but not the least, I extend my salutations to my parents, **Shri Mukesh Kamboj** and **Smt. Rama Kamboj**, they have been epitome of inspiration for me. I also thanks my big brother **Sachin kamboj, Gaurav kamboj** sweet sister **Anupriya Kamboj** and **Ankita Kamboj**, who has always been supporting pillar during my hard days.

Ankit Kamboj

ABSTRACT

Climate change has a significant role on the available water resources. There is a large variability in the water availability in the Mahanadi basin. Therefore, there is a requirement to modify the present knowledge and methods in measures modification in water resources during this region. To analysis the climate change, CORDEX data of two RCMs at daily time step for two different climate RCP 4.5 and RCP 8.5 scenarios has been used which are respectively produced by IITM and SMHI. The Early century (2010-2039), Mid-century (2040-2069), and End century (2070-2099) with respect to Reference period (1973-2004) was used for climate data analysis under two climate scenarios. The result showed that each climate model showed variability in the projected climate. VIC hydrological model has been used for Normal long-term discharge simulation. Calibration and validation was done for two different periods. For future river discharge simulation, VIC calibrated model forced by climate model data was used to generate the runoff scenarios. The result show large change in simulated runoff under the future climate scenarios RCP 4.5 and RCP 8.5 respectively. The results obtained from this study showed surface runoff is more sensitive to the changes in surface temperature and precipitation. Moreover, it was found that the change in stream flow and surface runoff are more effected due to change in precipitation rather than air temperature.

CONTENTS

LIST OF FIGURES

LIST OF TABLES

LIST OF ABBREVIATIONS

VIC	Variable Infiltration Capacity Model
RCPs	Representative Concentration Pathways
CORDEXs	Coordinated Regional climate Downscaling Experiment
CMIP5	Couple Model Intercomparison Project phase 5
IITM	Indian Institute of Tropical Meteorology
SMHI	Swedish Meteorological and Hydrological Institute
RCM	Regional Circulation Model
GCM	Global Circulation Model
SWAT	Soil Water Assessment Tool
LULC	Land Use Land Cover
DEM	Digital Elevation Model
ISRO-GBP	Indian Space Research Organisation Geosphere Biosphere Programme
NBSS & LUP	National Bureau of Soil Survey and Land Use Planning
WRIS	Water Resource Information System of India
LAI	Leaf Area Index

CHAPTER-1

INTRODUCTION

1.1 Background

Water is a standout amongst the most imperative, non-conventional resources on earth's crust. It is essential for all dimensions of life such as mankind, animal, plants, microorganism etc. On earth's surface, water is accessible in various forms and area such as on the surface, in the air, oceans, below the ground. It has been found that nearly 2.5% of the earth's water is freshwater available mainly in frozen state as glacier and ice sheet [Oki and Shinjiro, 2006]. About 96% of liquid fresh water can be found underground and remaining is available on the surface or in the air. India has about 4% of worlds freshwater available from rivers, stream, lakes, wetland, ground aquifer etc. India ranks among the top ten water rich countries having a broad network of river, which include twelve major river system and number of small river and streams. The Ganga-Brahmaputra and Indus system being the largest, as they drain around 40% of the available surface water from the Himalayan watershed to the ocean.

Because of quick increment in population of India and the need to fulfill national demand of water for various purposes, the pressure on available water resources has increased manifold in last few decades. This has lead to one of the biggest environmental concern for human mankind. While facilitating the quantity of water for daily need has reached critical situations at various places of India, equally critical is the continuous deterioration of its available quality. The quality of freshwater is being deteriorated due to several reasons, the most important being human induced pollution by industries, contaminates from cites and intensive agricultural activates. Ground water aquifers have also been found to be depleting in many parts of India leading the overall water crisis.

Expanded centralization of ozone depleting substances in the climate, have added to the woes of water availability. This increased concentration of greenhouse gases in the atmosphere is because of both natural and anthropogenic sources that causes variation in the internal atmosphere temperature of lower atmosphere. Changes in lower atmospheric climate condition are one of the main causes of the climate change that are taking place currently. Variation in the composition of atmospheric gases causes to continuously trap the heat that radiates from the earth and insulates the earth.

Climate change is visible in the increase in the extraordinary climate condition as warmth waves, floods, earthquakes, cyclones, and droughts with unfailing regularity all over the

globe. India has started to witness such extreme weather condition since last few years. The examples include Uttarakhand disaster 2013, Mumbai flood 2005, and Orissa cyclone 2017. So to avoid the problems resulting from climate change, its assessment, monitoring and management by employing integrated use of climate models and hydrological models becomes essential form the adaptation point of view.

1.2 Climate Modeling

Since the arrival of Intergovernmental Panel on Climate Change (IPCC's) the AR5, 4 representative centration pathways have been characterized as a reason for long haul and close term atmosphere demonstrating tests in the atmosphere displaying network (van Vuuren et al., 2011b). The four RCPs together traverse the scope of radiative constraining qualities for the year 2100 as found in writing, from 2.6 to 8.5 Wm^2 (Table 1.1). Atmosphere display utilize the time arrangement of future radiative constraining from the four RCPs for their atmosphere demonstrating investigations to create atmosphere situations. The announcements of RCPs enable atmosphere modelers to continue with tests in parallel to the improvement of outflow and financial situations (Moss et al., 2010). The four chose RCPs incorporate one moderation situation (RCP2.6), two medium adjustment situations (RCP4.5/RCP6) and one high pattern emanation situation (RCP8.5) (van Vuuren et al., 2011b).

Table 1. 1 Description and visualization of the four representative concentration pathways (RCPs) (Source: van Vuuren et al., 2011b)

S.no.	RCP	Description
1	RCP 8.5	Rising radiative forcing pathway leading to 8.5 Wm2(~1370ppm co2 eq) by 2100
2	RCP 6	Stabilization without overshoot pathways to 6Wm2(~850ppm co2 eq) at stabilization after 2100
3	RCP 4.5	Stabilization without overshoot pathways to 4Wm2(~650ppm co2 eq) at stabilization after 2100
4	RCP 2.6	Peak in radiative forcing at ~3Wm2(~490ppm co2 eq) before 2100 and then decline (the selected pathway decline to 2.6Wm2 by 2100

Since the 4 RCPs are thought to be illustrative of radiative constraining that can be normal by 2100, every one of them are, hypothetically, considered with rise to likelihood to be incorporated into environmental change affect thinks about. In any case, in environmental change affect ponders there is typically a tradeoff in what number of RCPs and what number of atmosphere models to be incorporated inside the accessible time and assets, while in the meantime having the capacity of creating powerful and solid outcomes.

In the vicinity of 1996 and the arrival of the IPCC's 5th appraisal report in 2013 (IPCC, 2013), the IPCC utilized an alternate arrangement of future situations, consolidating principle statistic, monetary and innovative main thrusts with future ozone depleting substance emanations. A broad depiction of this prior age of situations can be found in the IPCC's exceptional write about outflow situations [IPCC, 2000].

1.2.1 Types of Climate Models

Climate modelling employs two models at different spatial resolution. General circulation models (GCM) are wide range of climate models where they simulate large scale circulations patterns (e.g., pressure and geo potential heights) at spatial resolution ranging between 250-500 km. Regional circulations models (RCM) simulate at regional scale at spatial resolution ranging between 10-50 km. In practice, climate change studies require high spatial resolution information, especially in hydrological models to predict the future change. Data from GCM is forced to downscale at a very high spatial resolution through RCM models for further analysis.

The present cutting edge GCMs are sorted out in the fifth Coupled Model Intercomparison Project (CMIP5) document [Taylor et al., 2012], which were utilized as a premise by the IPCC for the age of its fifth Assessment Report. A comparative push to sort out the yield from RCMs is the CORDEX structure [Giorgi et al., 2009]. The prior CMIP3 [Meehl et al., 2007] file is the fundamental chronicle utilized for thinks about before the arrival of the CMIP5 file.

The quantities of GCMs accessible for climate change projections are expanding quickly. For instance, the CMIP3 chronicle [Meehl et al., 2007], which was utilized for the fourth IPCC Assessment Report [IPCC, 2007] contains yields from 25 diverse GCMs, though the CMIP5 file [Taylor et al., 2012], which was utilized for the fifth IPCC Assessment Report [IPCC, 2013], contains yields from 61 distinctive GCMs. These GCMs regularly have numerous

gathering individuals bringing about a considerably bigger number of accessible model runs. Considering the expansive number of accessible atmosphere models and imperatives in the accessible computational and HR, nitty-gritty environmental change affect thinks about, for example, depicted in this proposition, can exclude all projections.

The WCRP (World Climate Research Program) activity CORDEX (Coordinated Regional Downscaling Experiment; http://www.cordex.org/) has produced an outfit of local climate change projections for South Asia with high spatial determination (50 km) by downscaling a few CMIP5 AOGCM yields utilizing numerous RCMs.(Sanjay et al.(2017) assessed the intensity of the Coordinated Regional Downscaling Experiment RCMs in simulating the accepted qualities of the atmosphere across South Asia by examining the spatial inconstancy, design connection and root mean square blunder utilizing a Taylor chart. The outcomes demonstrated that the topographical dissemination of surface temperature and regular precipitation in the current atmosphere is unequivocally influenced by the decision of the RCM and limit conditions (i.e. driving AOGCMs), and the downscaled regular midpoints are not generally progressed.

Fundamentally the climate change affect examination considers require the atmosphere data with territorial subtle elements; anyway it is likewise vital to assess the best in class AOGCMs utilized as a part to downscale utilizing RCMs since the confinements and vulnerability natural in these worldwide atmosphere reenactments are unavoidably exchanged to the local outcomes (Sanjay et al.,2017). Consequently this examination utilizes CORDEX South Asia RCMs to examine their ability to represent the 20th century **change impact on hydrology of Mahanadi region** under different forcing conditions.

1.3 Climate Change Impact on Hydrology

Hydrological cycle plays very important role for all dimension of climate system commonly known as atmosphere, hydrosphere, lithosphere, cryosphere and biosphere. Hydrological cycle is one of the key processes where other atmospheric cycle operates. Single change in hydrological cycles components i.e. change in cloud cover and ice sheet influence the radiation budget of the earth and thus play to determine the climate response to increase greenhouse gas emissions (Bates et al. 2008) hence change in climate is interlinked to the hydrological cycle. Increase in surface temperature may lead to increase in water holding capacity of atmosphere and directly affects the hydrological cycle. Alteration in seasonal distribution, duration and magnitude in precipitation and evapotranspiration etc. are the common yet key changes in hydrological cycle as a result of climate change. Hydrological modeling is one of the most excellent techniques for climate change impact studies on hydrological cycle. In this hydrological models downscale all the information from climate models and distribute it on regional scale and studies the potential impact of climate change or a management measure on hydrological regime like river runoff, lake level or water available in an area.

1.4 Hydrological Modeling

Hydrological modelling is a better technique to assess climate change impact on water variability of single catchment or entire River basin using hydrological models. Mostly there are 2 types of models are existing: Physically and conceptual established hydrologic models. *Conceptual-lumped models* depend on basic course of action of a moderately modest number of netlike applied components and might be hope as one which midpoints inputs/yields over a zone and incorporates a few hydrological forms and their spatial fluctuation. Conceptual based information is not sufficient for climate change studies as these models require more modification and data enhancement than other type of models.

Physical based distribution models work on physical equations governed by physical laws. They assess unique fluctuation of special variability of computer file, boundary conditions, and watershed attributes for example Land use cover, soil characteristics, climate condition, emptying network, topography, earth science conditions i.e. Maximum. And

minimum temperature, precipitation, wind speed etc. From their physical premise, such models will mimic the whole spill over administration, giving various yields. In these models, exchange of mass, force and vitality zone unit is computed specifically from the overseeing incomplete differential condition of that territory unit and tackled utilizing exploitation numerical techniques, as a case the St. Venant conditions for surface stream, the semiotician equation for unsaturated zone flow and also the Boussinesq for water flow.

HEC-HMS (Hydrologic Engineering Centre-Hydrologic Modeling System) Variable infiltration Capacity model, MIKE-SHE, Soil and Water Assessment Tool, are some of the physically based distributed hydrologic models. In this study the land surface hydrological VIC has been used to assess the hydrological component simulation and climate change impact on study area.

1.5 Importance of Remote Sensing and GIS in Hydrological Modeling

Remote Sensing and GIS play a key role in hydrological modeling. Remote sensing and GIS hold a good arrangement of guarantee for hydrology, chiefly due to the possibility to look at areas and full watercourse watersheds instead of just points. Totally different input file varieties square measure needed to assess the hydrological modelling. This technique fulfils the need of many style of input file data sets required for modeling. Physical characteristics of the study space square measure driven principally by image process techniques and account topography mistreatment measuring instrument and Stereo pair's techniques. On the other hand, GIS has evolved as an extremely subtle knowledge of administration framework to place along and furthermore, heap the large knowledge usually needed for hydrological studies. Geographical information system gives the opportunities to mix knowledge from totally different sources and differing types, and this is utilised for hydrological studies when linkage with hydrological models is desired. All the topography data is well driven by Digital Elevation Model (DEM) equivalent to elevation, watershed drainage networks, and slope etc. GIS might be a critical mechanical assembly to be use in parameterization for enormous scale physically fundamentally based circulated models. During this study most of the input parameter files were generated using remote sensing and GIS based software.

1.6 Research Objectives

The principle target of this study is to assess the hydrological effects of climate change on water resource of the Mahanadi stream basin. To substantiate the fundamental target, the sub destinations are

- To set up hydrological model for the basin.
- To calibrate and validate the model for the basin.
- To analysis future meteorological parameters under different scenarios.
- To study impact of climate change on hydrological regime of the basin.

The flowchart of the methodology to achieve these following objectives is shown in Figure 1.1

Figure 1. 1 Methodology flowchart in the present research work

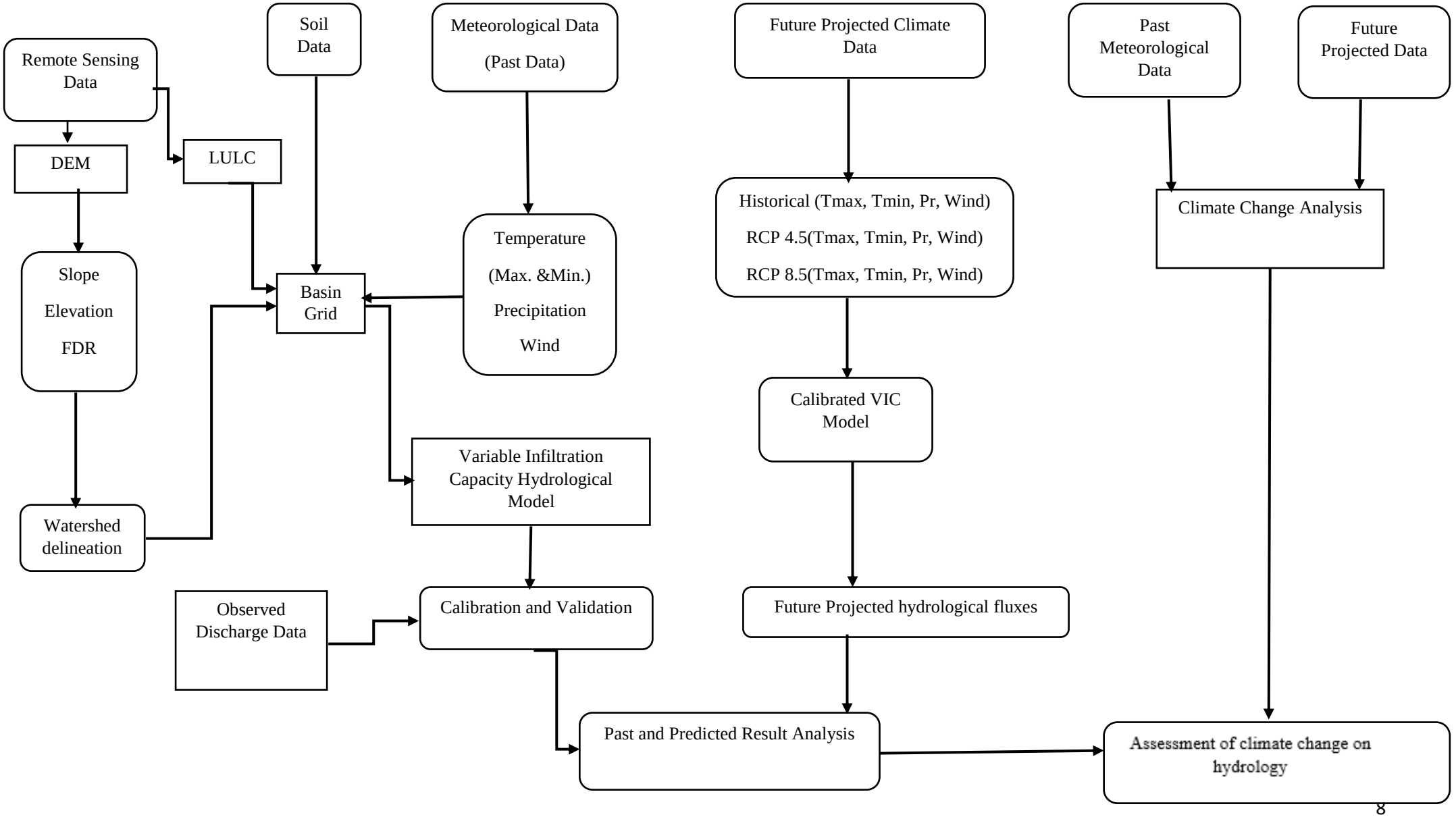

CHAPTER-2

LITERATURE REVIEW

This section gives a short audit of writing on impact of climate change on hydrology of river basin and an overview of Variable Infiltration Capacity model application as a hydrologic model keeping in view their utility in the proposed study. This chapter also includes the model overviews.

2.1 Climate Change and Water Resource

Bajracharya et al., (2018) studied the impact of climate change on the hydrology of the Kaligandaki basin (Nepal). In this study Representative Concentration Pathways Scenarios (RCP4.5 and RCP8.5) of General Circulation Models (GCM) which is ensemble of the Downscaled Coupled Model Intercomparison Projects (CMIP5) outputs were used to project the future changes in available water resources of the basin.

Sanjay et al., (2017) studied the mean precipitation and surface air temperature over the Hindu Kush Himalayan region. The study assessed multi climate model and multi-climate scenarios under climate change projection over the hilly sub region within Hindu Kush Himalyan areas for the near future (2036-2065) and far-future (2066-2095) periods.

Tan et al., (2017) studied the potential climate change effect on Kelantan River basin (north-eastern peninsular Malaysia). The Soil and Water Assessment Tool (SWAT) hydrological model under ensemble of Downscaled Coupled Model Intercomparison Projects (CMIP5) General Circulation Models (GCM) has been used. The 3 Representative Concentration Pathways Scenarios (RCP) used were 2.6, 4.5, 8.5 for different period 2015-2044 and 2045-2074.

Kumar et al., (2017) used bias-corrected Providing Regional Climates for Impact Studies data for projections. The study conclude increasing trends for yearly temperature and rainfall on the Upper Kharun Catchment (UKC) Chhattisgarh state in India. Hydrological assessment evaluated through Soil and Water Assessment Tool based on these projections, indicated over-corresponding runoff - precipitation and under-corresponding permeation precipitation connections.

Mishra et al., (2016) utilized bias corrected downscaled future climate projection and SWAT hydrological model on Indian sub-continental rivers. In the study, it was found that majority of the Indian sub-mainland waterway basin are anticipated to move towards hotter and wetter atmosphere later on.

Lutz et al., (2016) studied projected data of mean temperatures and rainfall on Indus, Ganga, and Brahmaputra (IGB) region. The studied revealed rise up to 3.5 ^{o}C for RCP4.5 scenarios and 6.3^{o}C for RCP 8.5 scenarios. Similarly, projected rainfall was found to rise by 3% to 37% under RCP4.5 and RCP 8.5 scenarios respectively.

D.Yun et al., (2015) studied the climate change effect on Pearl River in South China. Main objective of this studies were to show seasonal discharge and extreme flows under RCP 4.5 and RCP 8.5 emissions scenarios forcing conditions. Variable infiltration hydrological model (VIC) was used for this assessment.

Qiao et al., (2014) used dynamically and statistically downscaled climate projection to estimate the impact of climate change on water availability, ecosystem water quality. The hydrological model VIC is used to assess the climate change and hydrological components at Oologah Lake basin in China. The examination and correlation demonstrated that the powerfully downscaled projection catching better precipitation estimation as contrasted and the measurably downscaled projections, and the yearly water accessibility (runoff, precipitation, and base flow) projections were found to increase by 3–4%.

Garg et al., (2013) considered theoretical scenario– based effect appraisal of environmental change on spillover capability of a basin. Here an endeavor was made to abuse the abilities of a variable-infiltration capacity limit large scale hydrological model to recreate the Satluj stream basin in India. It was discovered that a slight change in atmosphere may cause colossal contrasts in the hydrological administration of the basin.

Chen et al., (2012) used different downscaling techniques like GCMs and hydrological models to assess and compared the differences in water balance simulations. The investigation reason that the re-enacted spill overs indicate fluctuation for the same GCM when utilizing precipitation gave by various factual downscaling models as the contribution to the hydrological models.

Gosain et al., (2011) studied the IPCC emission scenarios projection A1B for water resources of different river systems in India. They observed an uncertainty in the Indian River

system. Some river shows the increase in the water resources availability and while decrease in others.

Mishra et al., (2010) assessed the hydrological suggestions as a results of the climate change and land use land cover arrangement. Anticipated and memorable land utilize cover information alongside watched meteorological compelling information (1983 – 2007) were utilized to run the VIC demonstrate over Wisconsin (USA). The present LULC data was related along the projected (2030) land use cover info. The land transformed model (LTM) has been used to generate the projected land use cover. It was watched, the change of forested territory to agricultural land generate the expansion in surface drainage, latent heat, base stream and decline in evapo-transpiration.

2.2 Hydrological Modeling using VIC Model

Garg et al., (2017) studied LULC revolution impact on hydrology of Pennar stream watershed (India) using Variable Infiltration Capacity (VIC) Hydrological model. They presumed that all LULC classes indicate critical change between years 1985, 1995 and 2005 LULC.

H. Narendra et al., (2017) applied, the VIC model, over the 108780km^2 Tekra catchment which is a piece of Godavari river watershed (India). In this study, the performance assessment of VIC model was made in simulating the hydrology of the large catchment area.

S Zhou et al., (2014) employed VIC three layer hydrological model to the Baohe River basin with an objective to simulate earthbound hydrological forms for the whole basin. The study revealed that VIC three layer model simulated better along the observed data but underestimated the observed peak flows significantly.

Liu et al., (2013) utilized the VIC model to contemplate the land utilize and climate change over Qingyi stream watershed (China). The investigation inferred that the effect of climate change on the hydrological procedure is more conspicuous than the land utilize changes.

Garg et al., (2012) used Variable Infiltration Capacity hydrological models in Asan River watershed of Dehradun city and observed an increase in runoff due to urbanization.

Dadhwal et al., (2010) study the hydrological components of the Mahanadi basin (India). In this study, utilized the VIC hydrological model to assess the hydrology of the river stream. The main objective was to study the impact of lulc revolution of basin stream networks. Surface overflow was reenacted for the year 1972, 1985 and 2003 to measure the

progressions certain occurred because of progress in spatial change. An expansion by 4.53% in the yearly stream was seen at Mundali (Mahanadi) basin outlets from 1972 to 2003.

Liang et al., (2003) proposed another philosophy to depict the dynamic connection amongst ground and surface water. The new parameterization combined with VIC-three layers demonstrate named as VIC- ground accounted the ramifications of the cooperation on hydrological factors, for example, overflow, evapo-transpiration, soil dampness and revive. The outcomes underlined that the aggressive trade between the ground and surface water hydrology impacts the soil dampness and surface transitions essentially, which justified quick consideration.

From the above literature showed that, several studies have been made to assess the climate change impact on hydrology. Most of the study used CMIP5 multi-GCM model data to assess the climate change impact on water resource under different GHG climate scenarios. Assessment of surface air temperature and precipitation has been also predicted using different climate data (Sanjay et al., 2017, Lutz et al., 2016) under RCP 4.5 and RCP 8.5 scenarios. In most of the study, different technique has been used for downscaling and generated the hypothetical climate scenarios (Garg et al., 2013, Chen et al., 2012, Qiao et al., 2014). Similarly above literature show the importance of VIC model in hydrological modeling. The writing for the most part allude to acknowledgment of the VIC display in various perspective on water asset, for example, effect of LULC change (Garg et al., 2017, Liu et al., 2013, Garg et al., 2012, Dadhwal et al., 2010) on watershed. Therefore motivated from the above literature, the objective of this study has been carryout under three main steps. Firstly VIC model has been set up for Mahanadi Basin. Calibration and validation has been done for historical simulation. Secondly, change in precipitation and temperature based on three 30-years periods was done for climate data analysis. And for climate change impact assement, climate forcing driven from the output of four different climate models was used as meteorological forcing for calibrated hydrological model.

.

CHAPTER - 3

STUDY AREA

3.1 Overview of the Mahanadi Basin

Mahanadi is the biggest basin in India which contribute about 4.28% of the aggregate topographical territory of the nation. Mahanadi basin degree lies in Chhattisgarh and Odisha and furthermore covers little parts of Jharkhand, Maharashtra, and Madhya Pradesh conditions of India. The Mahanadi basin lies between scopes of 19^0 20' North to 23^0 35' North and longitudes of 80^0 30' East to 86^0 50' East (Figure 3.1). The aggregate catchment zone of Mahanadi basin covers 139681.51 sq. km. It is additionally peninsular stream which come after Godavari basin as far as water accessibility. (Source-India wris)

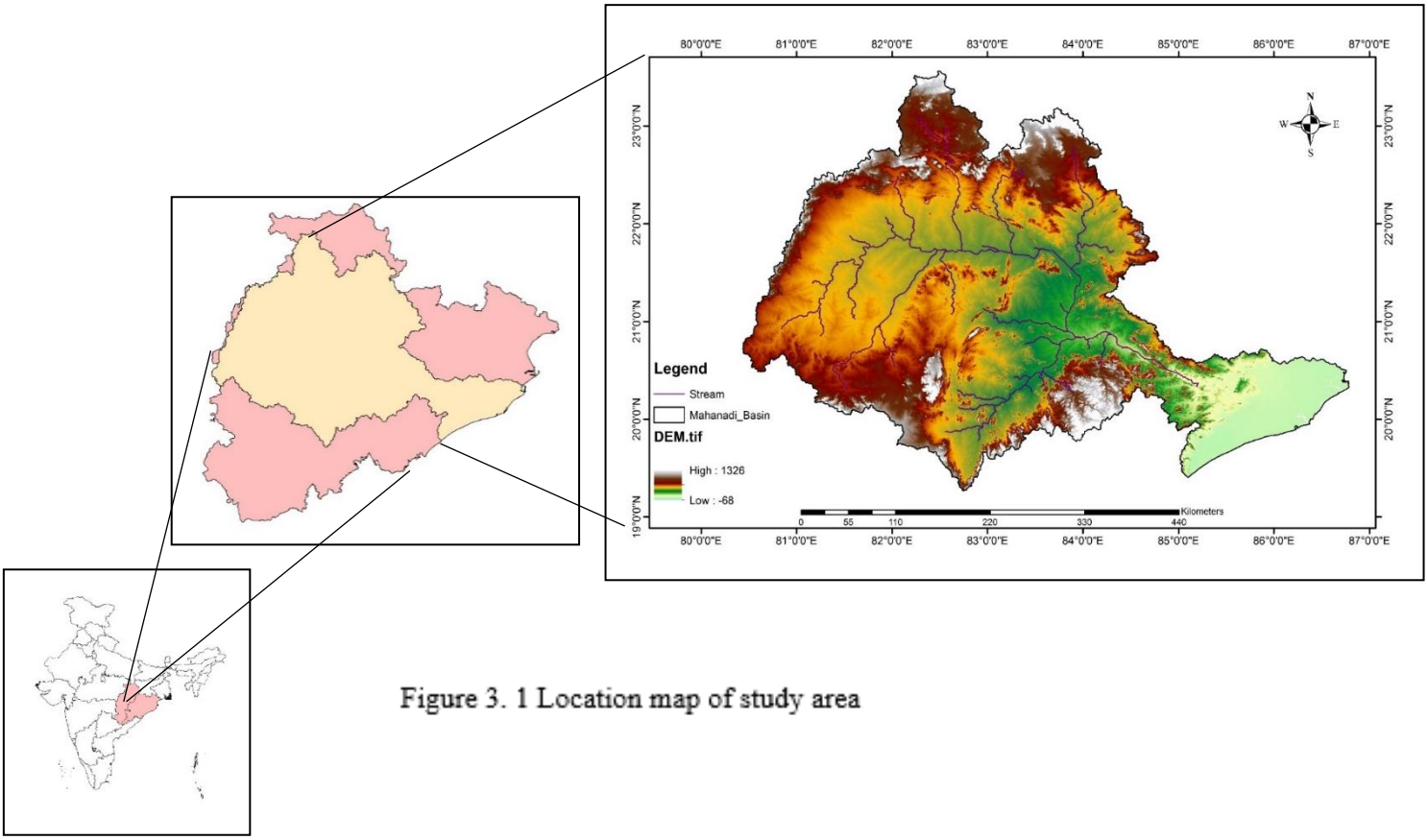

Figure 3. 1 Location map of study area

3.2 Climate Condition

Mahanadi keep tropical type of monsoon condition. It mainly experiences four distinct types of monsoon namely the cold climate, the hot climate, the southwest monsoon and the post monsoon. 90% of rainfall is receives during monsoon periods. For the most part, the southwest rainstorm sets by the center of June over the whole basin and stays dynamic till the finish of September. Tornado conditions are additionally shaped due scattering arrangement in Bay of Bengal and achieve overwhelming precipitation and coming about surge and devastation condition. The mean day by day least temperature differs from 7°C to 12°C, amid the cold period and the mean every day most extreme temperature fluctuates from 42.9°C to 45.5°C, amid the long stretch of May (source-India wris).

3.3 River System

Mahanadi have broad stream network system that begins from a tiny low portion at a rise of 457m above mean ocean level, 6km far from Farsiya of Dhamtari district of Chhattisgarh (India wris). Over the span of its cross, it depletes genuinely enormous regions of Orissa, Chhattisgarh and some little regions in the territory of Maharashtra and Jharkhand. The three noteworthy tributaries especially the Seonath and furthermore the Ib on the left bank and the Tel on the correct bank together constitute about 46.63% of the aggregate catchment territory of the waterway Mahanadi. The Tel is the second biggest stream of Mahanadi River and it likewise depletes 4 locale of Orissa specifically Balangir, Koraput, and Phulbhani, Kalahandi. The third largest tributary of Mahanadi is Lb., ascends in Raigarh region to Chhattisgarh. It depletes in locale of Chhattisgarh, to be specific Raigarh and areas of Orissa, especially Sambalpur, Jharsuguda and Sundergarh.

3.4 Land Use Land Cover (LULC)

LULC map of study area has derived from ISRO-GPB of year 2005 having 14 classes in the basin. Major portion is covered by cropland and deciduous broad leaf forest. Two largest water bodies in the basin are Hirakud reservoir and Chilka Lake which can be easily identified on LULC map. Small portion of Mangrove forest cover the water bodies parts. Fallow land, mixed forest, shrub land, wasted land, barren land etc. are also found in Mahanadi basin. These LULC classes are shown in Figure 3.2.

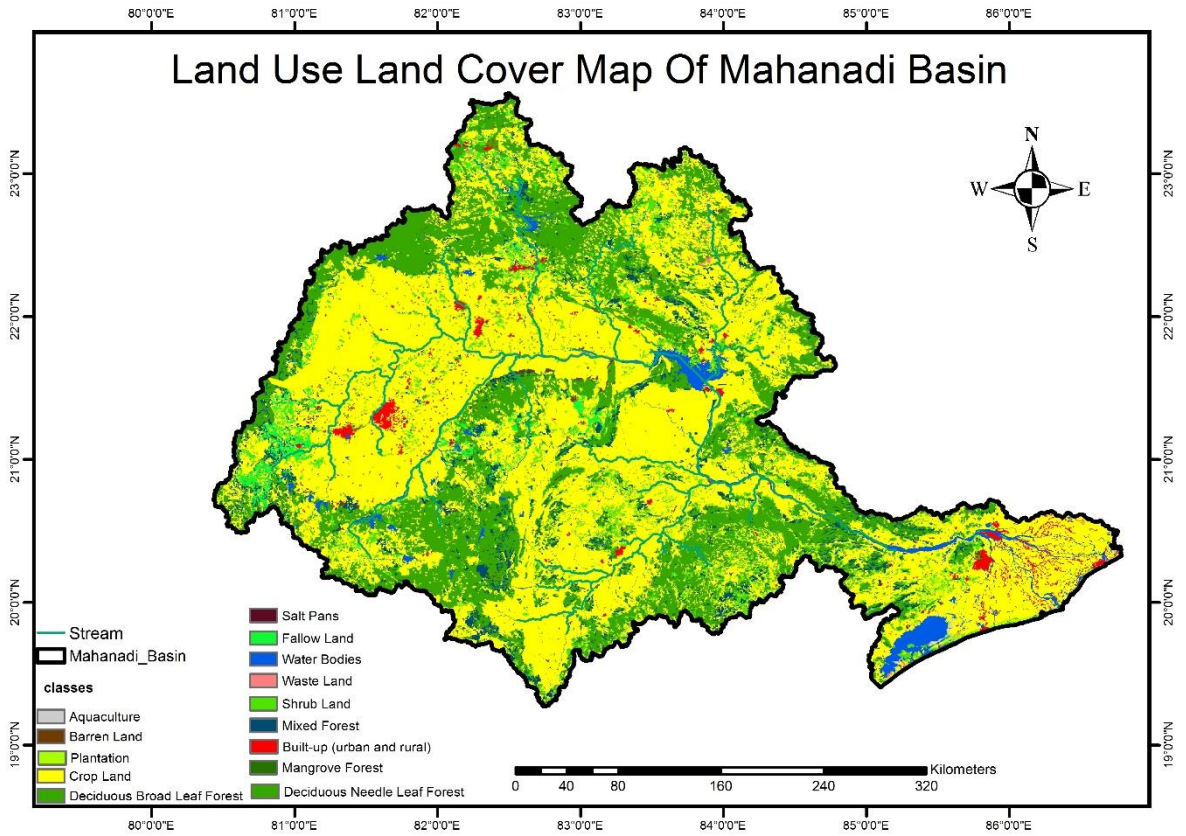

Figure 3. 1 LULC map of Mahanadi Basin

3.5 Physiography and Soil

Physiographical, the watershed is separated into below areas; specifically Eastern Ghats, Northern Plateau, the Coastal Plain, the Chhattisgarh fields and the erosional Plains. The initial 2 are bumpy districts. Focal inside plain is seaside plain which is crossed through stream and distributaries. Dirt prevails in the center and lower spans of the seepage direct and in the upstream channel rocks may likewise be found. The northern part of the area from Mayurbhanj to Sundargarh and Tel bowl contains red soil which is viewed as poor for vegetation. The Bolangir, Dhenkanal, Sambalpur contains the fruitful soil for agrarian reason. The Mahanadi-Tel basin in the northwestern bit of the locale is the most crowded and agronomically prosperous piece of the territory with reduced settlements. As per the rain components, the Eastern Ghats, the northern level, the focal tableland, and the beach front locales might be incorporated into the semi-sticky compose. (Source-India wris).

CHAPTER-4

MATERIALS AND METHOD

This chapter describes the various datasets used to generate input parameter files to set up VIC (Variable Infiltration Capacity) hydrological model. Climate data analysis for future designated centuries, have also been mentioned. The way to deal with survey the effect of climate change on the watershed is likewise examined.

4.1 Description of the Model

Overview of VIC Model

VIC model is a macro scale, semi-distributed & physically based hydrological model which design to represent hydrological fluxes, surface energy furthermore shape of different spatial resolution from large watershed to the whole globe (Liang, et al. 1994) (Liang, et al. 1996). This model was created to work on LINUX and UNIX platforms. It models both water and energy balances. VIC figures the vertical vitality and dampness motion in grid cell in view of particular at every matrix cell considering soil properties and vegetation scope (Liang, et al. 1994). It also incorporates the portrayal of sub matrix changeability in soil penetration capacity and allows multiple vegetation classes within the same grid cell.

VIC requires mainly 4 inputs such as rainfall, minimum & maximum daily temperature and wind speed. This different process like infiltration, base flow, and runoff are calculated by various empirical equations. Infiltration from other sources like rivers, recharge structures and seepage are not considered because in VIC, water penetrate through grid only not from the atmosphere. The infiltration information was combined with baseflow calculations derived from the model to understand how much of the infiltrated water is being lost. From this, the recharge potential of the study area was calculated.

The Basic feature of VIC is as follows:

1. The basin surface is displayed as a network of extensive (>1km), level, regular cells and sub-framework heterogeneity (e.g. height, land cover) is dealt with by means of statistical distribution.

2. Inputs are time arrangement of day by day or sub-day by day meteorological drivers (e.g. surface temperature, cloud fraction, wind speed, precipitation).

3. The water, atmosphere-land fluxes and vitality adjusts at the land surface, are calculated at a day by day or sub-every day time step.

4. Simply enter by water in a system of grid by methods for the air.

5. Grid cells are mimicked autonomously of each other, and whole simulation is kept running for every grid cell independently, 1 grid cell at once, instead of, for each time step, circling over all network grid.

6. Meteorological information for every grid (for the whole simulation time frame) are perused from a record particular to that network cell.

VIC can be run for water balance, energy balance, and frozen soil conditions or can be calibrated specifically for the area of interest. The parameters required for each type of study changes, but the model is very versatile and gives results for a wide range of scenarios.

4.1.2 Input Files for VIC

VIC requires different types of inputs into the grid for the model to give results. The grid can be created using QGIS or ArcGIS software's, after which different attributes of the study area need to be added into the grid.

The most important information is the Rungrid, which tells the model whether a particular grid lies in the study area or not. Other attributes include Lat/Long of the centroid of the grid, Area, Soil texture in each layer, Elevation of each grid, Slope of each grid, Rainfall in each grid and the Flow Direction. Elevation, slope, and rainfall values are calculated using the mean values within each grid, and the soil texture class and flow direction are calculated using majority values in each grid.

Further, different types of files, in ASCII format or .csv format are need to calibrate the model. These include-

The Global Parameter File- This tells the model two things; (1) names of the parameters files, their locations and types of formats and (2) characterizes the worldwide parameters of the simulation known as "run time" choices.

Meteorological parameter files- The daily and sub-daily meteorological variable parameters inputs for rainfall, temperature, humidity etc. can be used. There is flexibility in the number and combination of variables it can use.

Soil parameter files- This contains information about different soil parameters for each textural class described in your study area.

Vegetation library- This describes different types of LULC types in the area, and different properties of each LULC class for each month of the year.

Vegetation parameter files- Using the vegetation library, we can calculate the vegetation parameters of different classes within each grid of the run grid. This includes landcover types, fractional areas, rooting depths and seasonal LAI (Leaf Area Index).

For more detail refers to the appendix 1

4.2 VIC Tool

This tool is particularly create to prepare the input parameters file for VIC Model. The essential capacity performed by the device is classified as takes after:

- Composition of soil parameter file.
- Composition of vegetation parameters file.
- Meteorological forcing

4.3. Data Set Used in the Study

4.3.1 Digital Elevation Model

The advanced height model of Shuttle Radar Topographic Mission (SRTM) with 30m determination is utilized as a part of this investigation. This DEM was gained from USGS – Earth Explorer (https://earthexplorer.usgs.gov/) to delineate the watershed boundary and other required watershed property. Apart from it, the DEM has been used for extracting the topography information. The DEM showing highest elevation value over Mahanadi Basin is 1326m and lowest elevation value is -68m as shown in Figure 3.1

4.3.2 Land Use Land Cover Map

The LULC map acquired from ISRO GBP (Indian Space Research Organisation Geosphere Biosphere Programme). The LULC map of year 2005 is used with the scale of 1:250,000 in this study. This LULC map having around 14 classes of LULC. Figure 3.2 shows the LULC map of Mahanadi Basin for the year of 2005.

4.3.3 Soil Map

The soil map is taken from NBSS & LUP (National Bureau of Soil Survey and Land Use Planning) with the extend of 1: 250000. The soil texture information and other relevant stuff was derive from the map as shown in Figure 4.1.

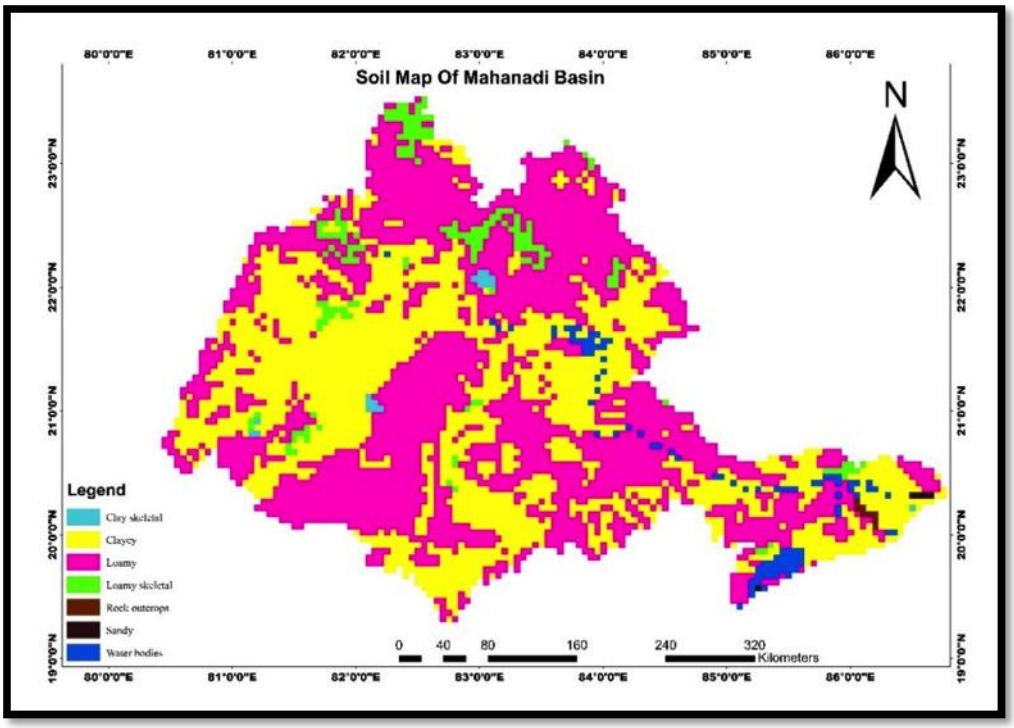

Figure 4. 1 Soil texture map of Mahanadi Basin

4.3.4 Discharge Data

Observed data is downloaded from India WRIS for outlet station Tikapara. This data gives the gauge discharge data (Cusec) in daily timescale for period 1973-2013. This is the discharge stations of Mahanadi Basin which has been considered for calibration and validation.

4.3.5 Observed and Future Meteorological Data

Observed constantly meteorological forcing were acquire from IMD (Indian Meteorological Department) for the period from 1951-2013. Max and Min temperature at 1^0x1^0 spatial resolution and 0.25^0 0.25^0 precipitations, wind direction, cloud fraction were taken as meteorological variable.

For projected future climate change impact assessment studies in the present study, bias corrected CORDEX data (https://esg-dn1.nsc.liu.se/search/cordex/) available at 50km spatial resolution for RCMs over the domain of south Asia was used. In this study the two

downscaled RCM (IITM-RegCM4-4, SMHI-RCA4) outputs of two different GCM model data CCCma-CanESM2, NOAA-GFDL-GFDL-ESM2M ensemble of r1i1p1 is available on ESGF (Earth System Grid Federation), and both are provided by SMHI and CCCR-IITM, respectively. The future projection from 2006-2100 are forced with two RCP 4.5 , RCP 8.5 covering Mahanadi regime in Early century (2010-2039), Mid-century (2040-2069) , End century (2070-2100) were analyzed. The features of these CORDEX data which is used in this research are listed in Table 4.1 given below.

Table 4. 1 Description of CORDEXs experimental institute data as shown below.

CORDEX South Asia RCM	RCM Description	Contributing CORDEX Modeling Center	Driving CMIP5 AOGCM (see details at https://verc.enes.org/data/enes-model-data/cmip5/resolution)	Contributing CMIP5 Modeling Center
IITM-RegCM4 (6 ensemble members)	The Abdus Salam International Centre for Theoretical Physics (ICTP) Regional Climatic Model version 4 (RegCM4; Giorgi et al., 2012)	Centre for Climate Change Research (CCCR), Indian Institute of Tropical Meteorology (IITM), India	CCCma-CanESM2	Canadian Centre for Climate Modelling and Analysis (CCCma), Canada
			NOAA-GFDL-GFDL-ESM2M	National Oceanic and Atmospheric Administration (NOAA), Geophysical Fluid Dynamics Laboratory (GFDL), USA
SMHI-RCA4 (6 ensemble members)	Rossby Centre regional atmospheric model version 4 (RCA4; Samuelsson et al., 2011)	Rosssy Centre, Swedish Meteorological and Hydrological Institute (SMHI), Sweden	CCCma-CanESM2	Canadian Centre for Climate Modelling and Analysis (CCCma), Canada
			NOAA-GFDL-GFDL-ESM2M	National Oceanic and Atmospheric Administration (NOAA), Geophysical Fluid Dynamics Laboratory's (GFDL), USA

4.4 Software Used in Study

- Arc GIS 10.0.1
- ENVI
- QGIS
- VIC (Variable Infiltration Capacity model)
    a. VIC 4.0.6 (water balance) b. VIC Route 2.0
- VIC tool –v0.1 (IIRS/ISRO)
- MATLAB

4.5 Grid Preparation of Mahanadi Basin

The daily hydrological simulation has been carried out using VIC hydrological model on Mahanadi basin. For this, basin grid of 5km by 5km resolution has been prepared in which 14600 are total numbers of the grid and 5147 are active grid (fully under basin boundary). Grid map of Mahanadi is shown in Figure 4.2 below.

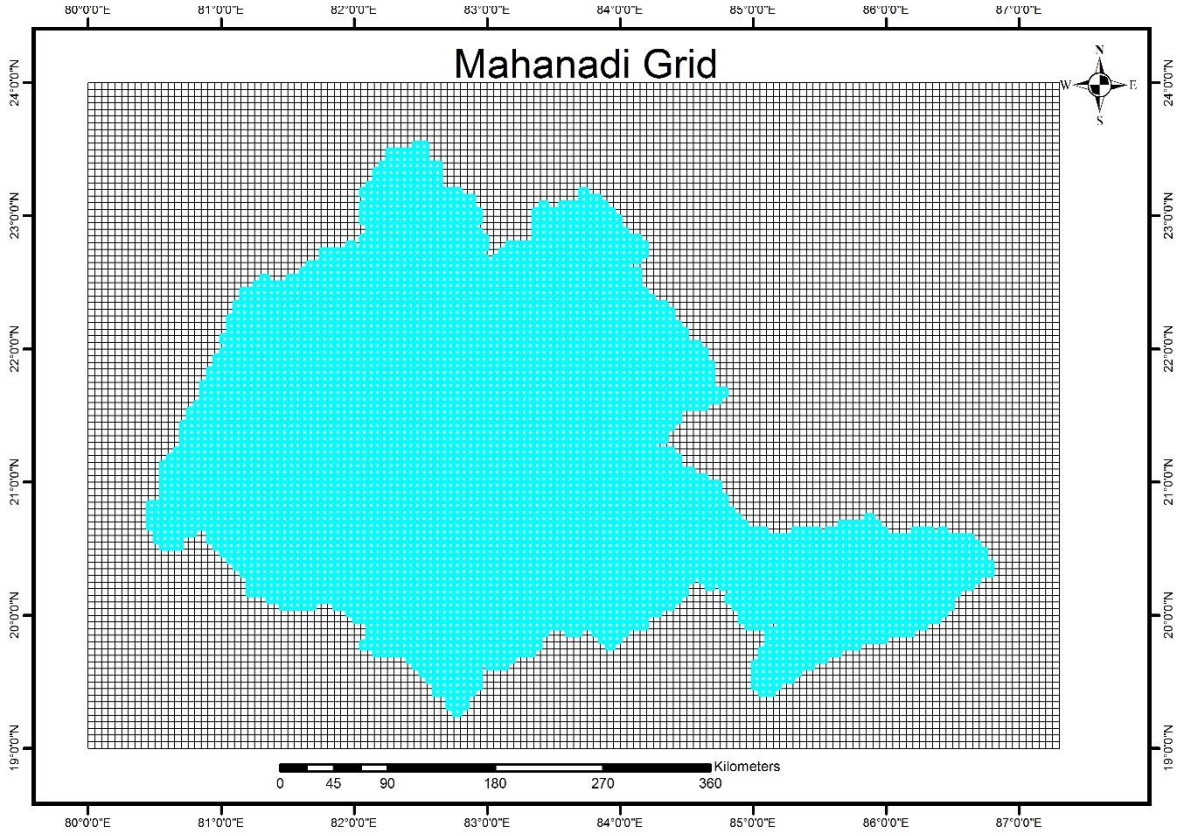

Figure 4. 2 Grid map of Mahanadi Basin (5x5km) resolution

4.6 Hydrological Model Parameterization

For the most part 4 essential information parameter records are needed for the VIC model. They are Vegetation parameter document, Soil parameter record, Vegetation Library record and forcing records. The information in these records is put away in the ASCII design.

4.7.1 Soil Parameter Files

The soil parameter document utilized by VIC depicts the exceptional soil stuff for every grid in the model space. It is likewise the primary record that recognizes which grid cell will be recreated, and what their scopes and longitudes are (which is utilized to discover the

compelling documents for the framework cells).The soil parameter file consists of two parts. In the first category soil parameter is not regulate but discover of the NBSS&LUB soil features. These parameter contain bulk density, saturated hydrologic conductivity, porosity etc. Another class of soil parameter is subjected to alignment in view of the understanding amongst mimicked and watched hydrograph. Parameter in this category includes infiltration capacitive curve Binf, baseflow parameter such as Ds, Dsmax, Ws and thickness of each layer. In the present study, the soil bulk density and texture information were calculated from the NBSS&LUP digitized soil map as shown in Figure. 4.3. http://www.hydro.washington.edu/Lettenmaier/Models/VIC/Documentation/SoilParam.shtml

Rungrid	Grid No.	Lat	Long	Binf	Ds	Dmax	Ws
1	1363	23.525	82.475	0.2	0.001	74.1571	0.9
1	1364	23.525	82.525	0.2	0.001	75.1228	0.9
1	1505	23.475	82.275	0.2	0.001	51.7589	0.9
1	1506	23.475	82.325	0.2	0.001	41.3575	0.9
1	1507	23.475	82.375	0.2	0.001	46.0169	0.9
1	1508	23.475	82.425	0.2	0.001	51.0312	0.9
1	1509	23.475	82.475	0.2	0.001	39.1467	0.9
1	1510	23.475	82.525	0.2	0.001	29.6395	0.9
1	1651	23.425	82.275	0.2	0.001	45.0308	0.9
1	1652	23.425	82.325	0.2	0.001	39.9834	0.9
1	1653	23.425	82.375	0.2	0.001	35.2819	0.9
1	1654	23.425	82.425	0.2	0.001	27.676	0.9
1	1655	23.425	82.475	0.2	0.001	24.8641	0.9
1	1656	23.425	82.525	0.2	0.001	22.7671	0.9
1	1796	23.375	82.225	0.2	0.001	33.8111	0.9
1	1797	23.375	82.275	0.2	0.001	32.7987	0.9
1	1798	23.375	82.325	0.2	0.001	34.6577	0.9
1	1799	23.375	82.375	0.2	0.001	33.5942	0.9
1	1800	23.375	82.425	0.2	0.001	27.9113	0.9
1	1801	23.375	82.475	0.2	0.001	25.3093	0.9
1	1802	23.375	82.525	0.2	0.001	23.7373	0.9
1	1803	23.375	82.575	0.2	0.001	35.0853	0.9
1	1804	23.375	82.625	0.2	0.001	59.0829	0.9
1	1941	23.325	82.175	0.2	0.001	27.2763	0.9
1	1942	23.325	82.225	0.2	0.001	35.4574	0.9
1	1943	23.325	82.275	0.2	0.001	41.4876	0.9
1	1944	23.325	82.325	0.2	0.001	45.7286	0.9
1	1945	23.325	82.375	0.2	0.001	45.4405	0.9
1	1946	23.325	82.425	0.2	0.001	41.29	0.9

Figure 4. 3 Sample of soil parameter file for VIC

4.7.2 Vegetation Parameter File

The vegetation library and vegetation parameter records were set up from Land cover maps created under ISRO-GBP LULC venture for the year 2005 at a 1:250,000 scale. From this information, the land cover composes and their divisions of the grid cell possessed by each are recognized, as depicted by Maurer et al. (2001) in the model space. The vegetative structure (from any land-cover grouping plan) relate to every grid cell is portrayed in vegetation parameter document which utilizes a similar framework cell numbering as the soil record. Pulling profundity for each LULC class is likewise determined, which empowers, shorter harvests and grasses draw dampness from the surface soil layers, and tree roots from the more profound soil layer.

LAI is the vital normal for the land cover that influences the VIC show hydrological recreation. The month to month mean LAI relating to every vegetation class has been identified from the MODIS (Moderate Resolution Imaging Spectroradiometer) information item on LAI (http://ladsweb.nascom.nasa.gov/information/search.html). The LAI esteems for a specific LULC class will change regularly; henceforth, intra-yearly varieties in vegetation qualities have been fused at month to month time scale utilizing month to month LAI for separate classes. The extra parameters including harshness length and relocation tallness (in m), design obstruction (in s/m), and least stomatal opposition (in s/m) for every vegetation tile were amassed in light of Global Land Data Assimilation System database (http://ldas.gsfc.nasa.gov/gldas/GLDASmapveg.php). This document cross-record every vegetation tile to the classes recorded in the vegetation library. Appendix 2, 3 demonstrates the overview of vegetation library and vegetation parameters records.

Grid No.	Vegetation Type	Classes Fraction	Root Depth
1363	3		
	2	0.05	0.1
	8	0.9225	0.1
	13	0.0275	0.1
1364	3		
	2	0.015	0.1
	8	0.97	0.1
	13	0.015	0.1
1505	3		
	2	0.005	0.1
	8	0.94	0.1
	13	0.055	0.1
1506	3		
	2	0.0225	0.1
	8	0.925	0.1
	13	0.0525	0.1
1507	1		
	8	1	0.1
1508	2		
	2	0.2925	0.1
	8	0.7075	0.1

Figure 4. 4 Sample of vegetation parameter file for VIC

4.7.3 Meteorological Forcing

Files contain different meteorological variable, which are mandatory for VIC hydrological model. Max and Min temperature, precipitation, wind speed, cloud fraction were taken as a meteorological forcing for hydrological simulation in this studies. Forcing information records assume imperative part in the model contribution to create every one of the output in both fully energy and water adjust methods of the model.

Table 4. 2 Overview of meteorological forcing

Variable Name	Units	Description
Tmax	Degree Celsius	Maximum temperature
Tmin	Degree Celsius	Minimum temperature
pr	Millimetre	Daily mean precipitation
Wind speed	Meter per second	Horizontal wind direction

4.8 Global Parameter files and Initial Model simulation

A Global control record where the fundamental data to determine different client inclinations and parameters was readied. It contains data like No. Of soil layers, Time duration i.e. start time, end time, meteorological variable temperature, Location of the info and output records, modes which are to be initiated and so forth. VIC source code was downloaded from the VIC site and the codes were unfastened and untared into neighbourhood source code catalog. At that point VIC was gathered utilizing gcc complier on Cygwin terminal. The code was ordered utilizing the make record incorporated into the document, by writing 'make'. The assembled code makes an executable entitled 'vicNl'. To start running the model, 'vicNl - g (global control record name)' was composed at the order provoke. Worldwide control parameters were adjusted by the info qualities and to initiate the water adjust. Notwithstanding that info and output way were indicated.

4.9 Preparation of Routing Input Parameter file

Generally five input parameter file are required to route the model. These include:

Flow direction file

Stream heading has been created utilizing SRTM DEM with a similar cell estimate as the spatial determination of matrix is 5*5km. To get flow directions HEC-HMS tool was used where all watershed delineation processes were performed. The flow direction obtained from DEM was converted according as VIC routing model as shown in Table 4.3. Once the change is done then it was converted in to the raster format and using conversion tool in arc toolbox (ArcGIS software) was converted to ASCII format for VIC routing model shown in Fig 4.5.

Table 4. 3 Comparison of flow direction notation

Direction	Flow direction code by convention	According to VIC source code
North	64	1
North-East	128	2
East	1	3
South-East	2	4
South	4	5
South-West	8	6
West	16	7
North-West	32	8

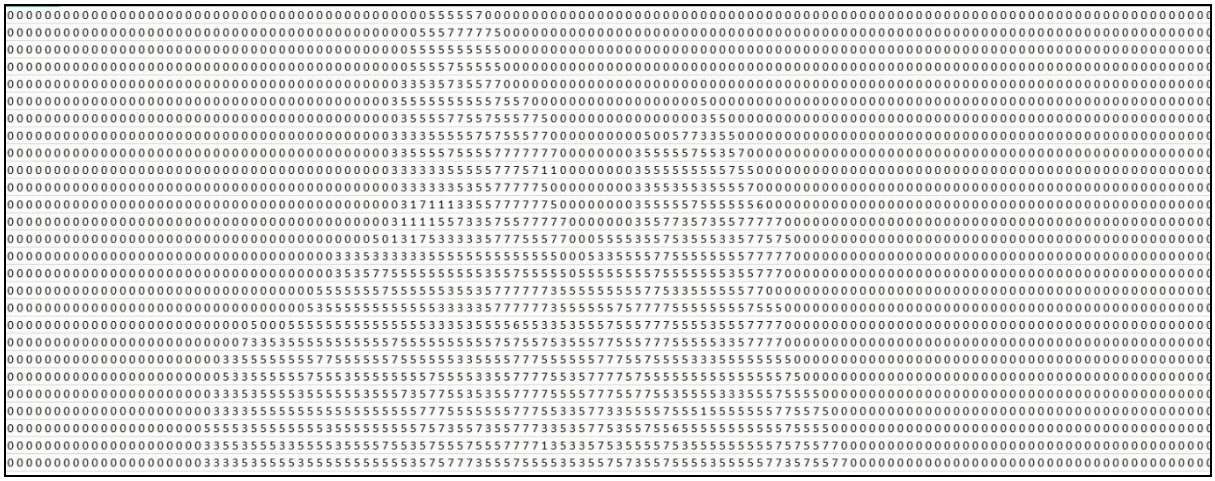

Figure 4. 5 Flow direction for VIC

Fraction file

Fraction file contains the fraction portion of those gird, which fall on edge of boundary of basin. Inside the basin its carry one and outside where inactive grids are assigned the zero values. Figure 4.6 shows the fraction file for its use in VIC model.

Figure 4. 6 Fraction file for VIC

Station location file

Station location file contain information about the located station for which calibration and validation would be done and they also contain information about the row and column of located station.

Unit hydrograph file

The Unit hydrograph record contains the grid cell drive reaction work whose entirety over every one of the months will dependably be equivalent to 1. Insight about the unit hydrograph has been specify in (http://www.hydro.washington.edu/Lettenmaier/Models/VIC/Documentation/Routing/RoutingInput.shtml#UH_ALLfile)

4.10 VIC Routing Model Run

Routing has been done on LINUX platform where different input files are require to route the model. Defeat source code was downloaded from the website and compiled using the make command. Input parameter like grid fluxes, fraction file, flow direction file, global parameter file and unit hydrograph, are require to route the model.

Routing model contain different time series discharge data of particular station which were mention in station file. These files are generally in ASCII format in Day, Month, Year in MM and Cubic Feet units.

4.11 Model Calibration and Validation

The observed and simulated discharges at the Tikapara gauging station were compared. The model was run from 1990-1995 under calibration made.

VIC model has been calibrated on the basis of two types of Parameter estimation:

a) Upper layer parameters adjustment
b) Bottom layer parameters adjustment

4.11.1 Upper Layer Parameters

These parameter adjustments bring change processes like infiltration or evaporation and are affected and in consequence these would cause variation on the runoff. These parameters are b_infiltration Soil depth_1 (b_inf) and soil depth_2.

1. b_inf - [>0 to ~0.4] it characterizes the state of the Variable Infiltration Capacity bend. It portrays the measure of accessible invasion limit as a component of relative immersed matrix cell territory. A higher estimation of bi gives bring down penetration and yields higher surface runoff (Gao et, al.2009).
2. Soil layer depth (b1, b2) - [between 0.1 to 1.5 meters] Soil profundity impacts numerous model factors. As a rule, for overflow contemplations, thicker soil profundities back off (baseflow overwhelmed) occasional pinnacle streams and increment the misfortune because of evapotranspiration. The most extreme soil dampness stockpiling limit is powerfully controlled by the difference in soil thickness. The thicker the dirt profundities are (bringing about more soil dampness put away in the dirt layers), the less spillover is created (Gao et, al.2009).

4.11.2 Bottom Layer Parameters

Generally these are base flow parameters that help to control base flow and also delay in runoff.

1. Ds - [>0 to 1] it is the part of Dsmax, where non-straight (quickly expanding) baseflow starts. On higher estimation of Ds, the baseflow become high and bring down water capacity in the soil layer.

2. Dsmax - [>0 to ~30, relies upon water powered conductivity] It is the most extreme baseflow parameter can happen from the least soil layer (in mm/day).

3. Ws - [>0 to 1]. It is the portion of the most extreme soil dampness (of the last layer of soil) site non-direct baseflow happens. Increase in Ws, water contents found to be increase and delay in runoff occurred.

The calibration parameters were adjusted as recommended, then the calibrated model was validated for data between periods 1996 to 2011. In this study, calibration was done taking into account above mention factors that affect the water balance components. Five parameters were changed several times for the period 1990-1995, and model was run again to see the changes, compare the discharge with observed data to see the change and processes repeated till the value become close to observed data.

4.12 Climate Data Impact Assessment Analysis

To assess the climate change impact, four climate model data has been used. IITM-CCCma-CanESM2, IITM-NOAA-GFDL-GFDL-ESM2M, SMHI-CCCma-CanESM2, SMHI-NOAA-GFDL-GFDL-ESM2M were observed to be most usually utilized climate model for climate change and hydrological studies. Data was in Netcdf format of spatial resolution 50x50km. This Netcdf files were converted to tiff format and projected to World Geodetic System (WGS) -1984 from rotated coordinated system. MATLAB platform were utilized to extract the values of maximum temperature, precipitation, wind speed and minimum temperature. A total of 126 years of climate prediction have been conducted for each climate scenario RCP4.5 and RCP 8.5 (1973–2099). This data of future scenarios RCP 4.5 and RCP 8.5 respectively were utilized to generate future meteorological forcing. The well calibrated and validated VIC hydrological model was then forced with this forcing keeping other parameters such as soil, LULC, topography same. To analyse the impact of climate change, the result were analysed for early centuries (2010-2039), mid-centuries (2040-2069) and end centuries (2070-2099). The long-term average of discharge of each century under consideration was compared to long term average of past i.e. period from 1973-2004. However, the analysis is based on three 30-year periods: reference period (1973–2004), Early century (2010-2039), Mid-century (2040-2069), and End-century (2070-2099). Average mean approach comparisons were used for projected change in precipitation and surface air temperature for estimated periods.

CHAPTER – 5

RESULTS AND DISCUSSION

In the present investigation, the climate change impact on hydrological regime of Mahanadi Basin has been assessed adapting the methodology described in previous chapter. VIC model has been setup for the entire Mahanadi Basin. Calibration and validation has been done on historical meteorological forcing. Then the future projected climate data has been analysed and the climate change impact on hydrology regime of the basis was assessed. The results obtained are discussed in the subsequent section of this chapter

5.1 VIC Model Set Up

The VIC has been used for simulation of discharge and to assess climate change impact on Mahanadi basin. To achieve the decided objectives, the entire basin has been discretized in grid of 5x5 km spatial resolution in which 5147 are the Rungrid (grids lies in the basin) and 14600 are total no. of grid. The grid preparation and all input parameter procedure has been discussed in previous chapter. The model is set up for entire basin taking the outlet at Tikapara.

5.1.1 Model Calibration

VIC model was setup and was calibrated using IMD forcing (1951-2013), in combination with monthly observed discharge data for discharge station describe in previous chapter. Observed discharge data were taken from India WRIS. Data is available on daily basis. Calibration was done on five years data on monthly basis from 1990-1995 and further the data of period from 1996-2011 was used for validation. Figure 5.1 show the VIC model simulation for the period of 1990-1995. The coefficient of determination show a fair agreement between the trends of simulated and observed stream flow record with a value of 0.80 at Tikapara. However, although R^2 value obtained was good (Figure 5.2), the peak discharge was not matching with the observed. Therefore, the model was re-calibrated. For calibration, five parameters were used to calibrate the model as discussed in the previous chapter. Trial and error calibration method was used and the calibrated values of $b_{inf,}$ Ds, Ws, Z1 and Z2 are shown in Table 5.1

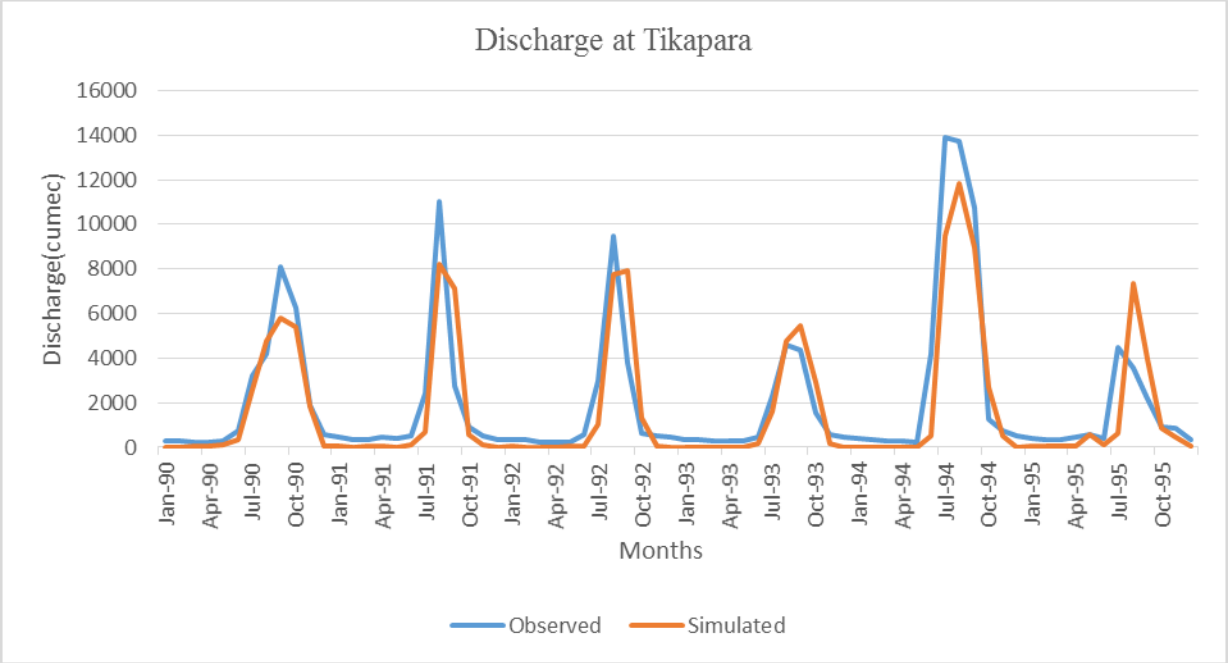

Figure 5. 1 Initial-calibration comparison of observed and simulated discharge (1990-1995)

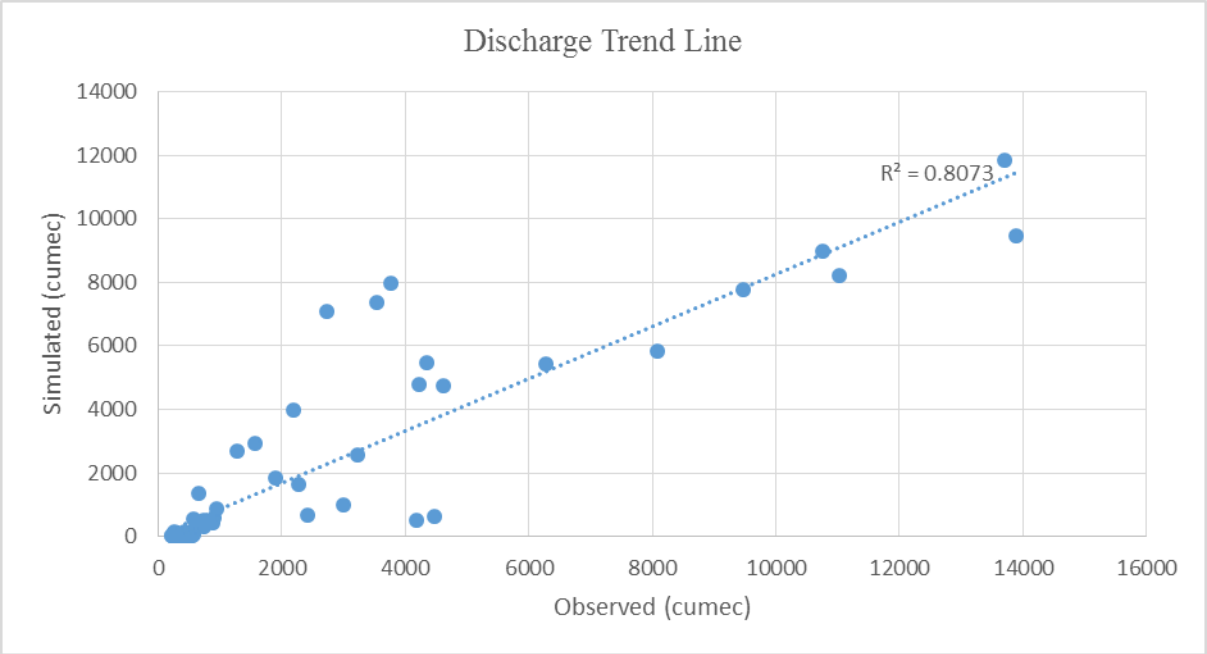

Figure 5. 2 Pre-calibration trend between observed and calibration at Tikapara

Table 5. 1 Calibrated value for model calibration parameter

Parameter	Range/value	Calibrated Value
b_{inf}	>0 to 0.4	0.2
Ds	>0 to 1	0.001
Ws	>0 to 1	0.9
Depth_1(Z1)	0.1-1.5	0.3
Depth_2(Z2)	0.1-1.5	0.7

Monthly hydrograph from 1990-1995 as shown in Figure 5.3 give better simulation after calibration. Best fitted calibrated value for calibration parameter are shown in the Table 5.1. The coefficients of determination (R^2) is now 0.81 for the Tikapara outlet. The model is now able to match the peak.

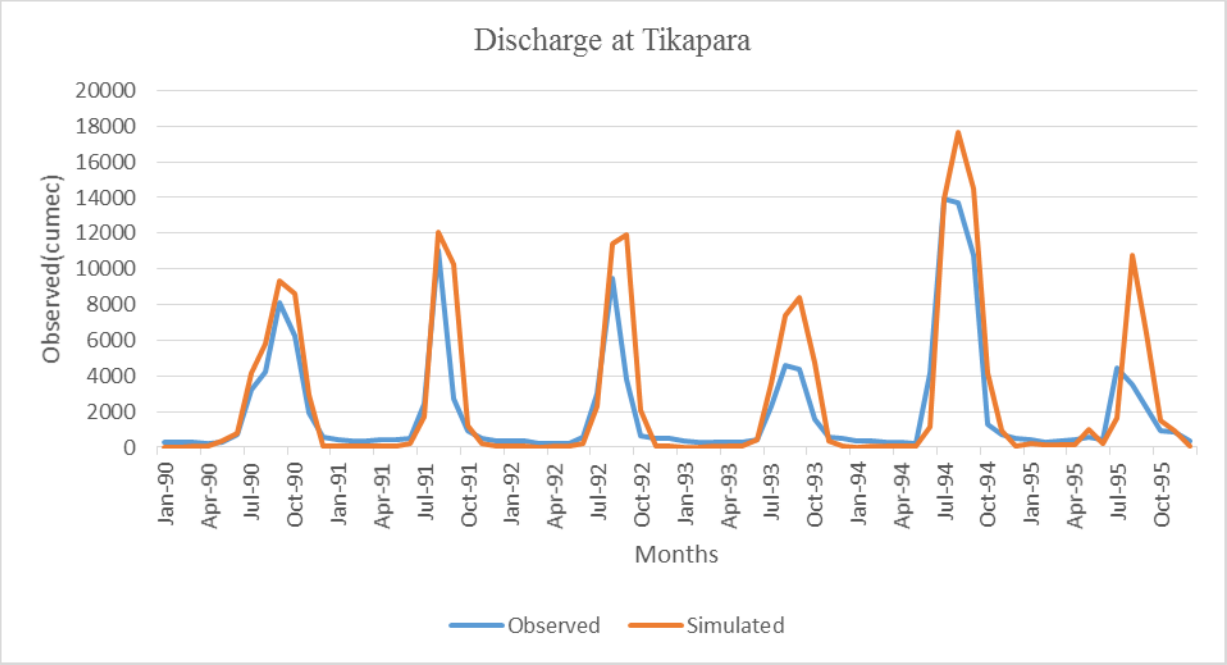

Figure 5. 3 Discharge comparison between observed and simulated at Tikapara

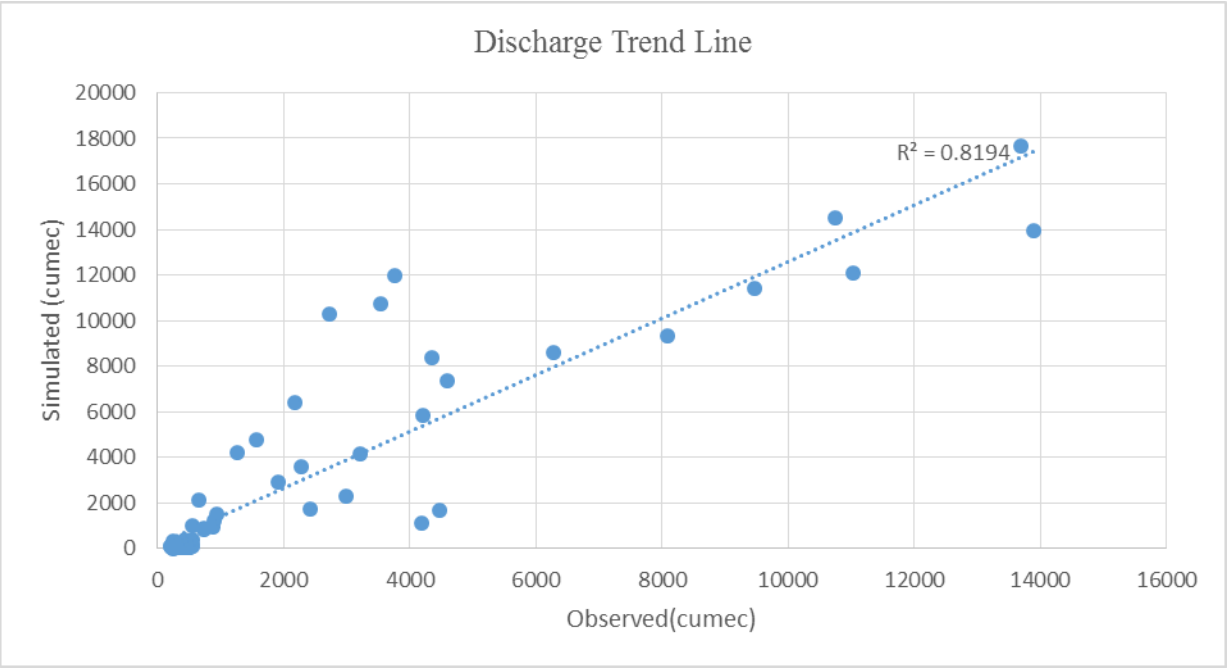

Figure 5. 4 Discharge trend between observed and simulated at Tikapara.

5.1.2 Model Validation

Validation is one of the important process for a calibrated model. For satisfactory, whether the value of calibrated parameter is best fitted or not, there is a need to validate the calibrated model. For validation period data should be different from the calibration. For validation of the model data of period 1996-2011 was used.

Model performance was found good at Tikapara during both calibration and validation for two different period. As in the present analysis the basin has been consider as virgin i.e. the any type of human intervention etc. has not been considered and therefore due to a slight overestimation in peaks is found to exist as compared to observed discharge during the validation as shown in Figure 5.5. And the coefficients of determination (R^2) is 0.77 for the Tikapara outlet as shown in Figure 5.6.

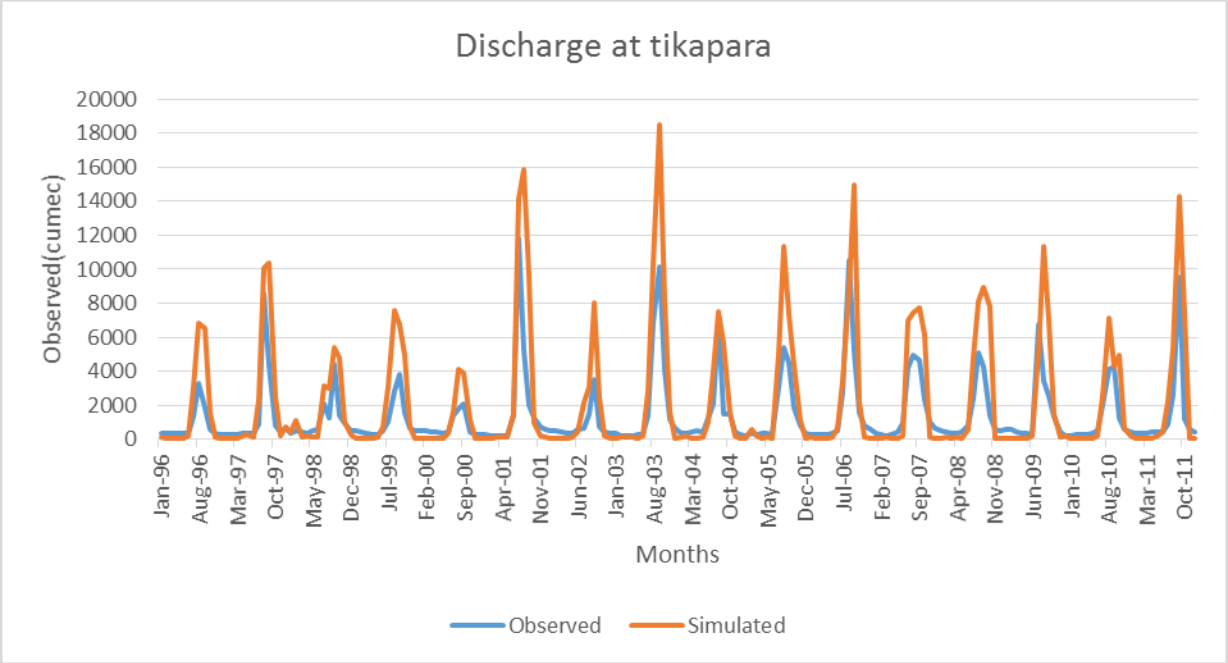

Figure 5. 5 Monthly discharge validation between observed and simulated at Tikapara for (1996-2011) period.

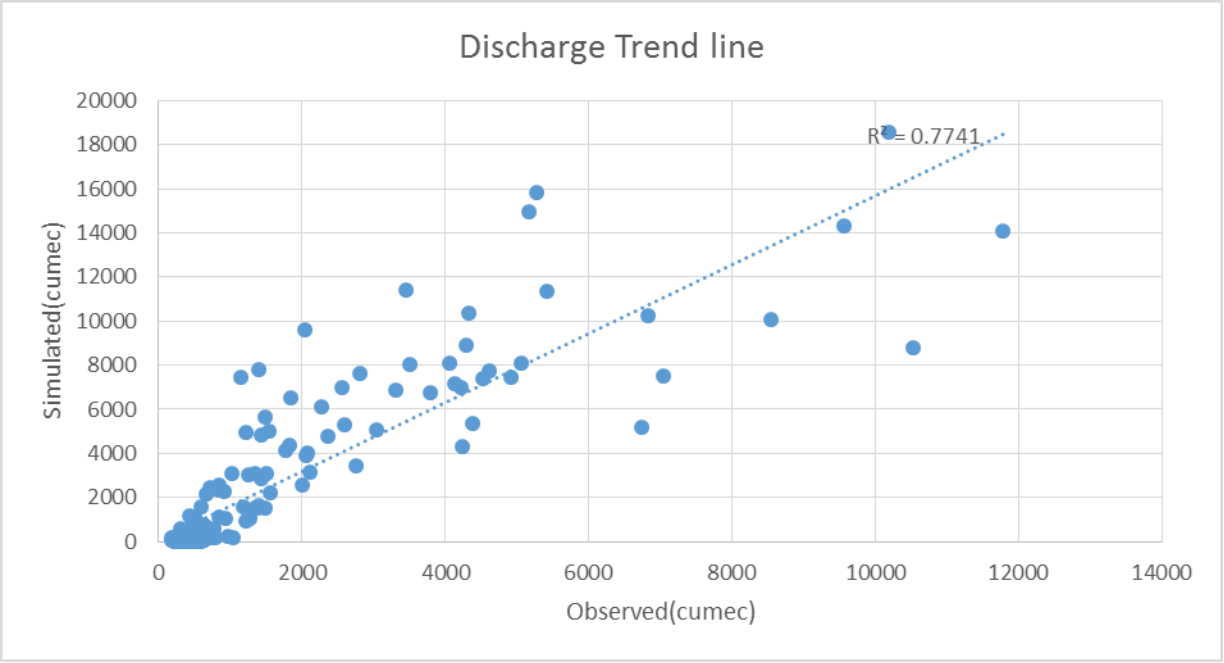

Figure 5. 6 Discharge trend between observed and simulated at Tikapara.

5.3 Future Climate Change Analysis

Long-term average mean calculation of Meteorological variable (Maximum temperature, Minimum temperature and precipitation). For three different centuries i.e. Early Century (2010-2039), Mid Century (2040-2069) and End Century (2070-2099) under the future climate RCP 4.5 and RCP 8.5 scenarios were obtained. Results shown that in each climate model, there is variation in the projected surface temperature and precipitation for all the period in both RCP 4.5 and RCP 8.5 scenarios.

IITM-CCCma-CanESM2 show variation in Tmax, Tmin and precipitation with Normal long-term (1973-2004) taken as reference period. Result show that, Early Century and Mid Century of RCP 4.5 and RCP 8.5 followed the same trend in maximum temperature as shown in Figure 5.7 (a) & (b). Figure 5.7(c) show that in the End Century period maximum temperature increased by 2.11% under RCP 4.5 and RCP 8.5. Where minimum temperature increased 10.64% and 19.32% in RCP 4.5 and in RCP 8.5 respectively with respect its reference period. Trend of minimum temperature under future climate RCP 4.5 and RCP 8.5 scenarios for all estimated periods are shown in Figure 5.7 (d), (e), (f).

In case of projected precipitation, reduction in precipitation intensity was found and peak shift toward June. It is clear from Figure 5.7 (g), (h), (I) that there is a reduction in intensity of precipitation for all estimated periods till to End Century (2070-2099) average precipitation increased by 17.02% in RCP 4.5 and 30.25% increase in RCP 8.5 with respect to Long-term normal (1973-2004) of reference periods Table(5.2) .

Less changes were observed, on comparing with Normal long-term meteorological data with future predicted climate data. Result showing that, IITM-NOAA-GFDL-GFDL-ESM2M predicted less change in maximum surface temperature and future precipitation for Mahanadi basin. Maximum temperature show slightly increase in End Century (2070-2099) period up to 1.022% in RCP 8.5 and low prediction were found in precipitation in all estimated periods under the projected future climate RCP 4.5 and RCP 8.5 scenarios. Significant change has been observed in minimum temperature where it increased by 0.05% in RCP 4.5 and 10.14% shown by RCP 8.5 as depicted in Table (5.3)

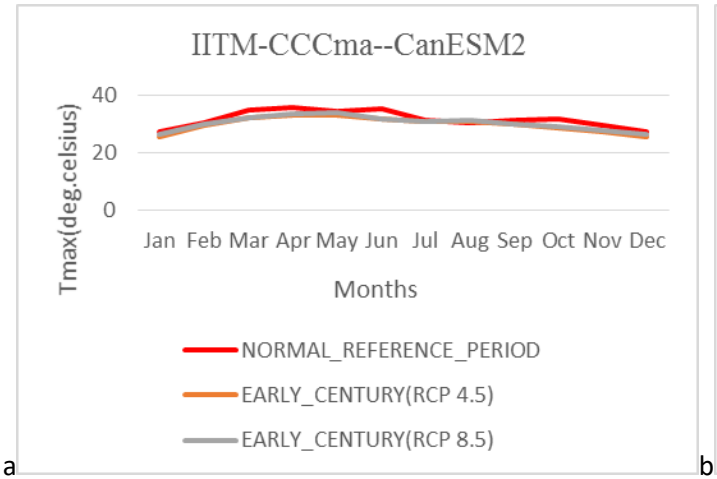
IITM-CCCma--CanESM2
Tmax(deg.celsius)
40
20
0
Jan Feb Mar Apr May Jun Jul Aug Sep Oct Nov Dec
Months
NORMAL_REFERENCE_PERIOD
EARLY_CENTURY(RCP 4.5)
EARLY_CENTURY(RCP 8.5)

a

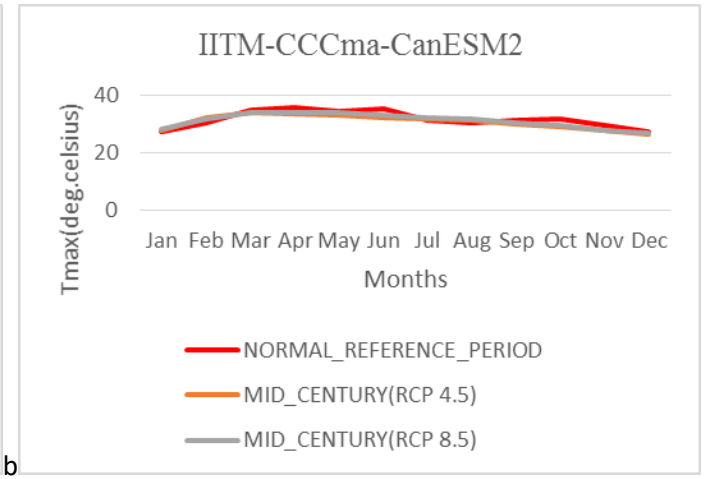
IITM-CCCma-CanESM2
Tmax(deg.celsius)
40
20
0
Jan Feb Mar Apr May Jun Jul Aug Sep Oct Nov Dec
Months
NORMAL_REFERENCE_PERIOD
MID_CENTURY(RCP 4.5)
MID_CENTURY(RCP 8.5)

b

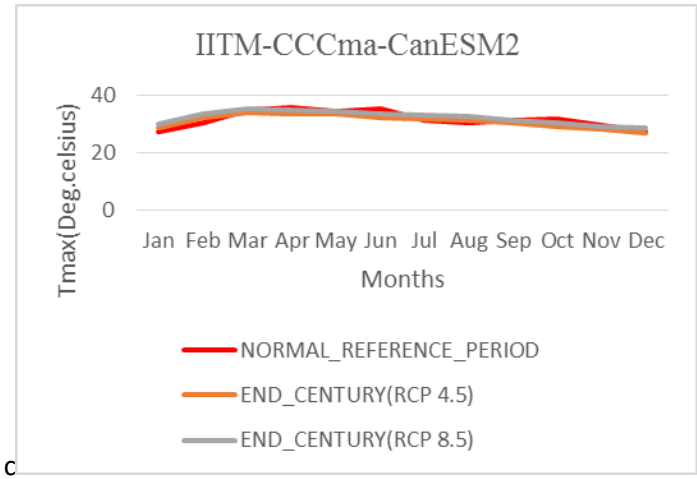
IITM-CCCma-CanESM2
Tmax(Deg.celsius)
40
20
0
Jan Feb Mar Apr May Jun Jul Aug Sep Oct Nov Dec
Months
NORMAL_REFERENCE_PERIOD
END_CENTURY(RCP 4.5)
END_CENTURY(RCP 8.5)

c

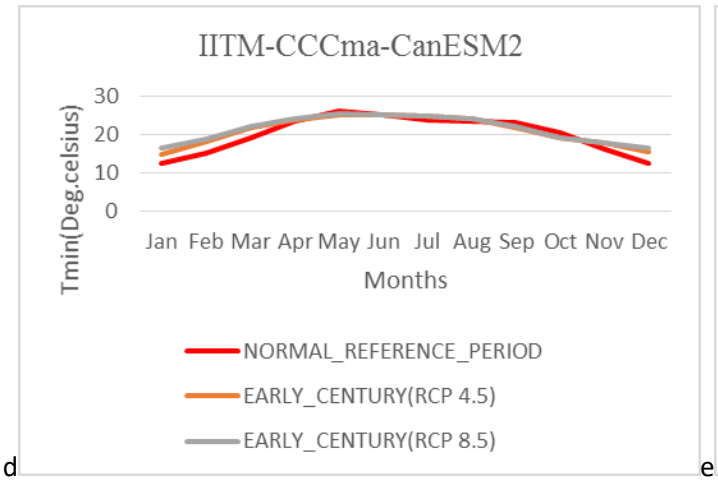
IITM-CCCma-CanESM2
Tmin(Deg.celsius)
30
20
10
0
Jan Feb Mar Apr May Jun Jul Aug Sep Oct Nov Dec
Months
NORMAL_REFERENCE_PERIOD
EARLY_CENTURY(RCP 4.5)
EARLY_CENTURY(RCP 8.5)

d

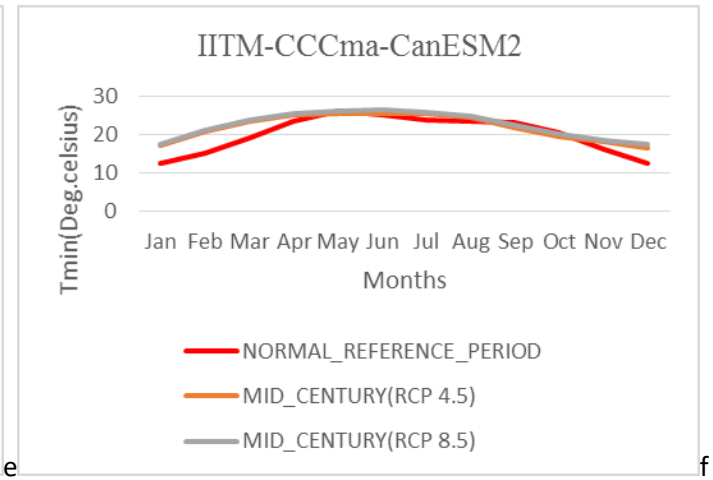
IITM-CCCma-CanESM2
Tmin(Deg.celsius)
30
20
10
0
Jan Feb Mar Apr May Jun Jul Aug Sep Oct Nov Dec
Months
NORMAL_REFERENCE_PERIOD
MID_CENTURY(RCP 4.5)
MID_CENTURY(RCP 8.5)

e

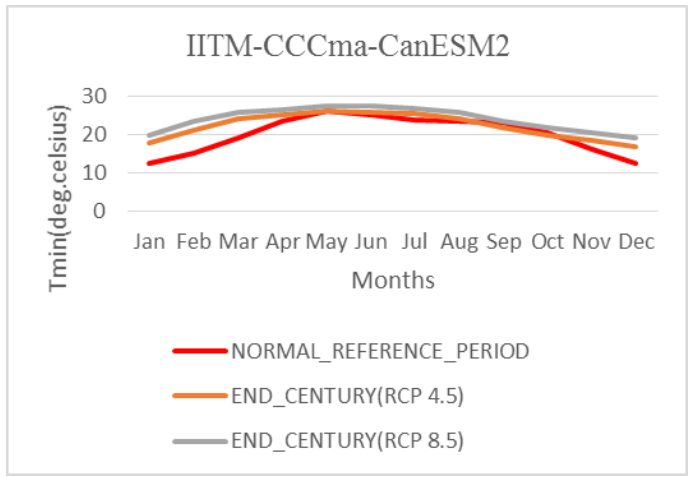
IITM-CCCma-CanESM2
Tmin(deg.celsius)
30
20
10
0
Jan Feb Mar Apr May Jun Jul Aug Sep Oct Nov Dec
Months
NORMAL_REFERENCE_PERIOD
END_CENTURY(RCP 4.5)
END_CENTURY(RCP 8.5)

f

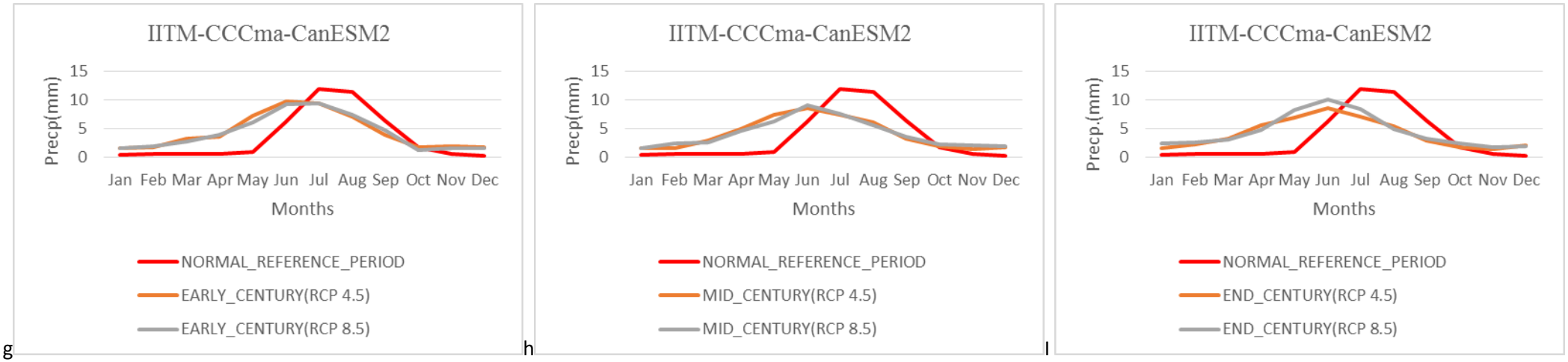

Figure 5. 7 (a-c) Tmax, (d-f) Tmin and (g-I) Pr average monthly comparison of IITM-CCCma-CanESM2 for all three centuries under future projected RCP 4.5 and RCP 8.5 scenarios against reference periods.

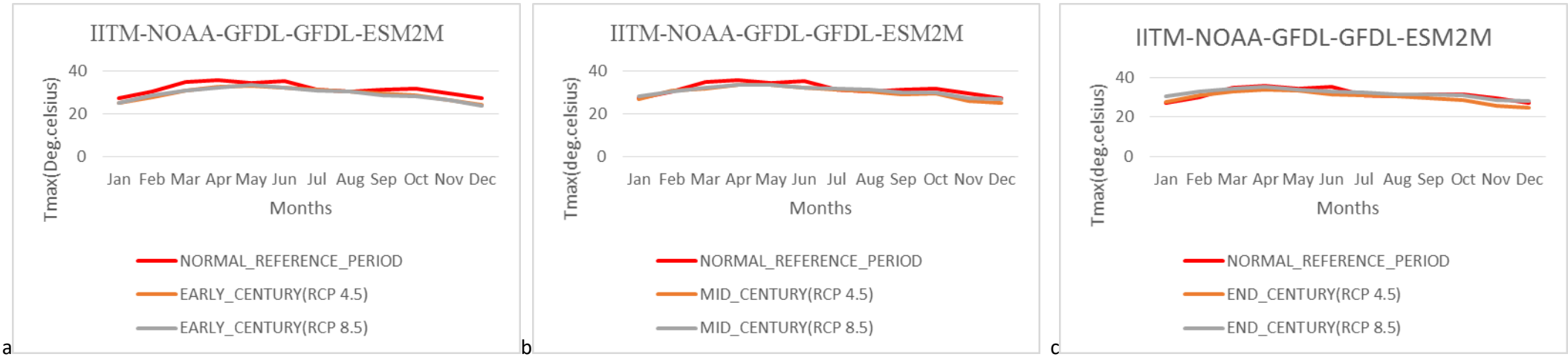

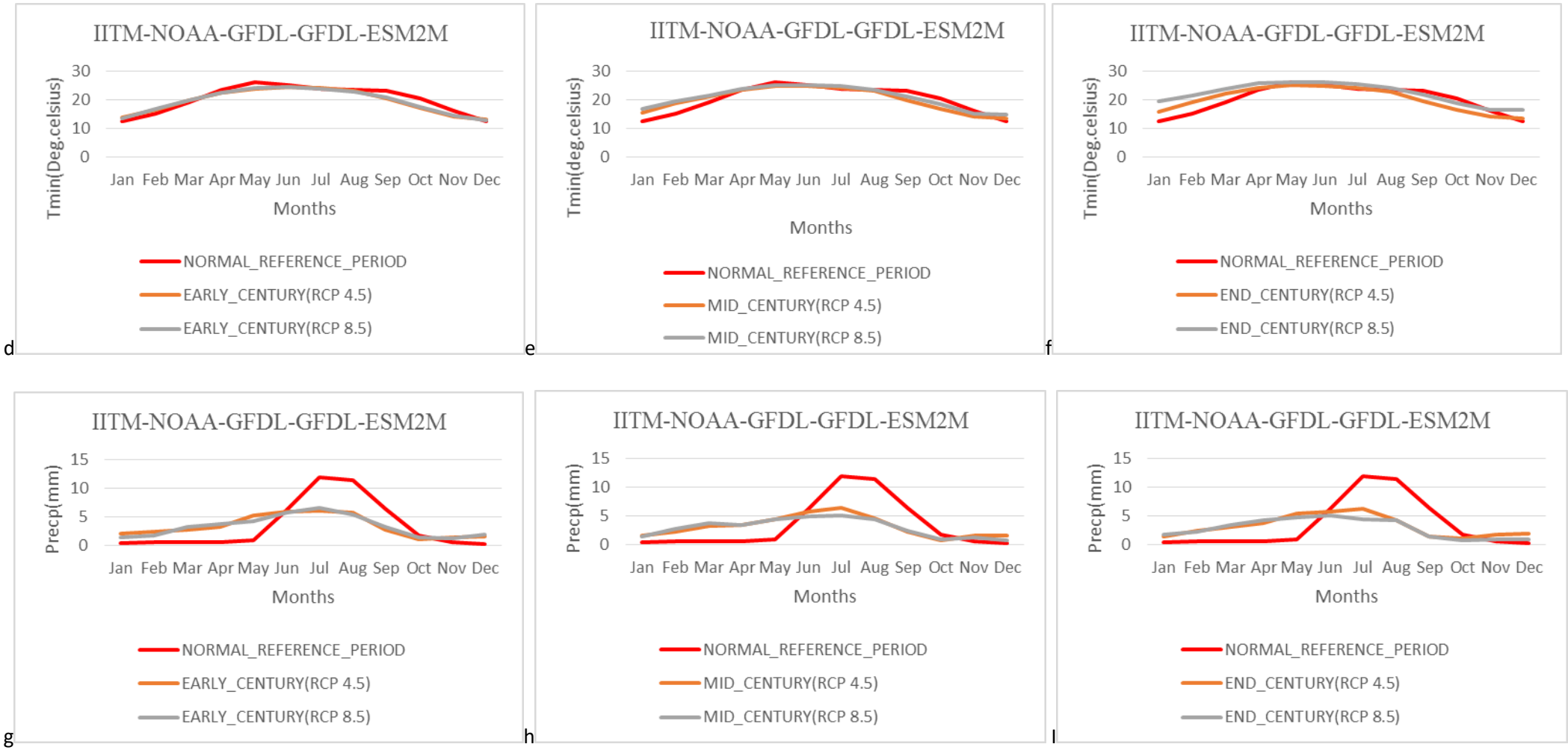

Figure 5. 8 (a-c) Tmax, (d-f) Tmin & (g-I) Pr average monthly comparison of future of IITM-NOAA-GFDL-GFDL-ESM2M for all three centuries under future projected RCP 4.5 and RCP 8.5 scenarios against reference periods.

SMHI-CCCma-CanESM2 and SMHI-NOAA-GFDL-GFDL-ESM2M were also used for prediction of future climate data. High maximum temperature trends were predicted in the End Century (2070-2099) by SMHI-CCCma-CanESM2M climate model. There is 15.62% increased maximum temperature RCP 8.5 and 11.15% increased for RCP 4.5 between 1973-2004 and 2070-2099 from Figure 5.9 (d). An increasing trend has been observed in minimum temperature where it increased by 20.13% for RCP 8.5 and 8.48% for RCP 4.5 between 1973-2004 and 2070-2099 respectively.

For precipitation, in RCP 4.5 the highest increase are projected for all three centuries. It is cleared from Figure 5.9 (g), to 5.9(I) that RCP 4.5 show high prediction in precipitation with Long-term normal of reference 1973-2004 periods. Monsoon peak is found to shifts towards August with high intensity. The RCP 8.5 show high prediction in precipitation with respect to the reference periods but low intensity was observed and average precipitation has been increase by 16.14 % with respect to RCP 4.5 Figure 5.9 (I) and Table (5.4). For the month of January the average precipitation indicate a decreasing trend, unchanged for February, slightly increase in precipitation for March and April and then high projection was observed from May to September and peaks was observed in month of August in RCP 4.5. Similar trend was followed for RCP 8.5 scenarios, where slightly less precipitation was predicted on comparison with RCP 4.5. Positive and negative projection of precipitation change was predicted for estimated period under the future climate RCP 4.5 and RCP 8.5 scenarios with respect to reference period.

SMHI-NOAA-GFDL-GFDL-ESM2M climate model predicted differently form SMHI-CCCma-CanESM2 under the future climate RCP4.5 and RCP 8.5 scenarios. Large uncertainty was predicted in averaged mean value in precipitation for all three century. From Figure. 5.10 (g) to 5.10 (I), an uncertainty were found as high precipitation has been started from April and reached to August. Maximum surface temperature has been increased by 2.53% in RCP 8.5, and a decrease of 2.62% in RCP 4.5 as shown in Figure 5.10(a), to 5.10(c) and Table (5.5). On the other side, minimum temperature was increased by 3.13% in RCP 8.5 and decreased by 6.22% in RCP 4.5 between End century (2070-2099) and reference (1973-2004) period.

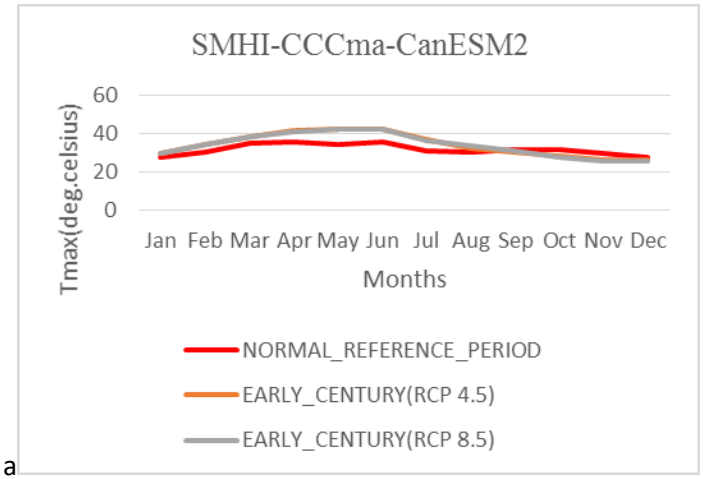
SMHI-CCCma-CanESM2
Tmax(deg.celsius)
60
40
20
0
Jan Feb Mar Apr May Jun Jul Aug Sep Oct Nov Dec
Months
NORMAL_REFERENCE_PERIOD
EARLY_CENTURY(RCP 4.5)
EARLY_CENTURY(RCP 8.5)

a

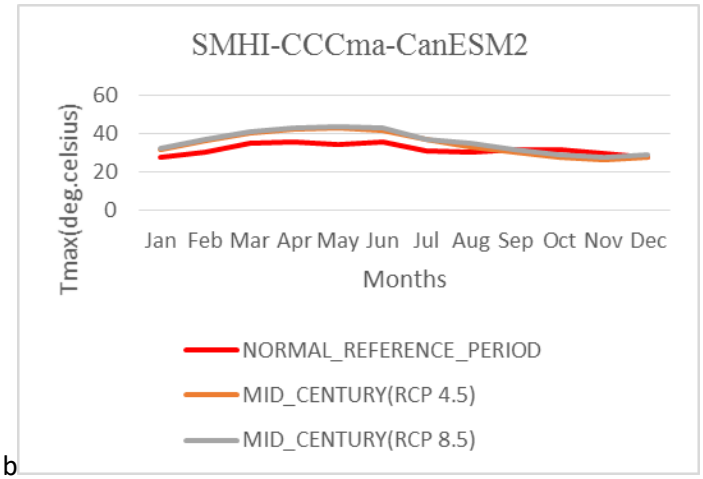
SMHI-CCCma-CanESM2
Tmax(deg.celsius)
60
40
20
0
Jan Feb Mar Apr May Jun Jul Aug Sep Oct Nov Dec
Months
NORMAL_REFERENCE_PERIOD
MID_CENTURY(RCP 4.5)
MID_CENTURY(RCP 8.5)

b

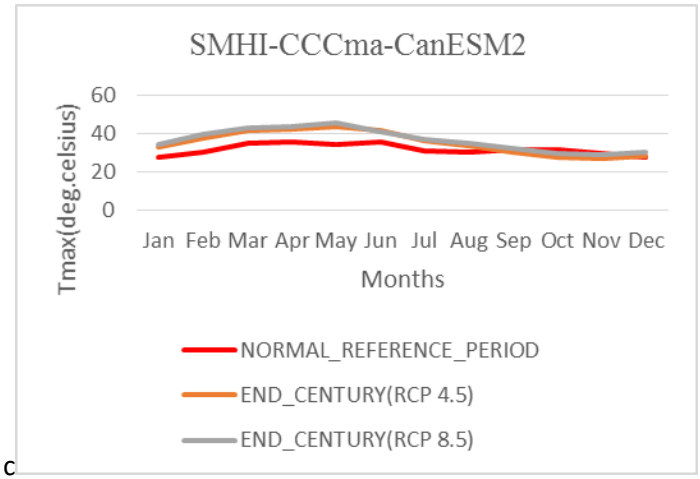
SMHI-CCCma-CanESM2
Tmax(deg.celsius)
60
40
20
0
Jan Feb Mar Apr May Jun Jul Aug Sep Oct Nov Dec
Months
NORMAL_REFERENCE_PERIOD
END_CENTURY(RCP 4.5)
END_CENTURY(RCP 8.5)

c

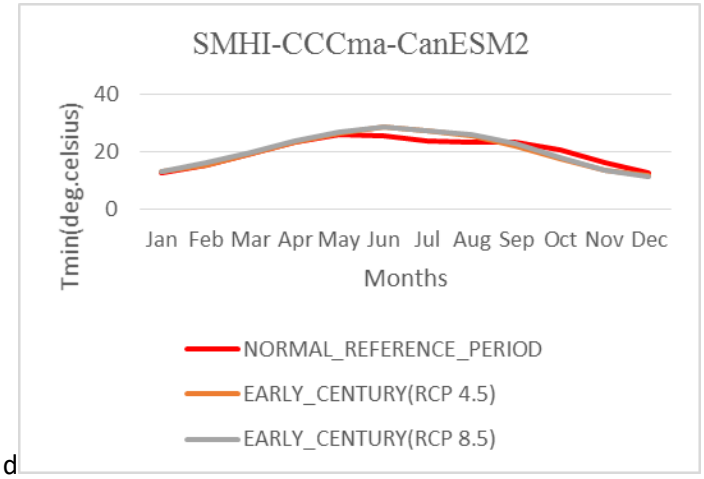
SMHI-CCCma-CanESM2
Tmin(deg.celsius)
40
20
0
Jan Feb Mar Apr May Jun Jul Aug Sep Oct Nov Dec
Months
NORMAL_REFERENCE_PERIOD
EARLY_CENTURY(RCP 4.5)
EARLY_CENTURY(RCP 8.5)

d

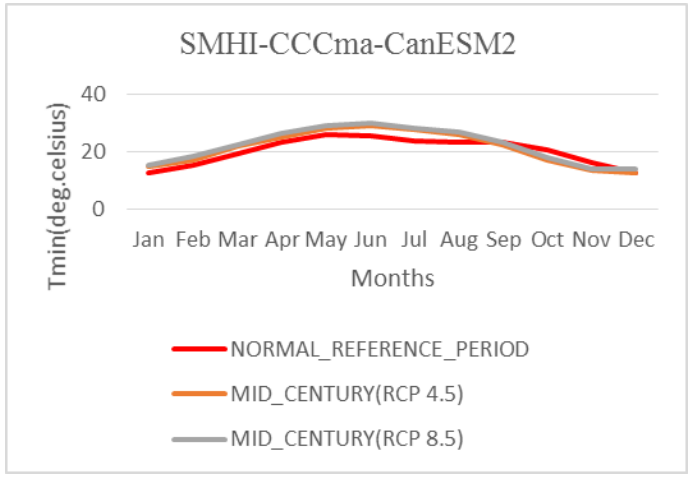
SMHI-CCCma-CanESM2
Tmin(deg.celsius)
40
20
0
Jan Feb Mar Apr May Jun Jul Aug Sep Oct Nov Dec
Months
NORMAL_REFERENCE_PERIOD
MID_CENTURY(RCP 4.5)
MID_CENTURY(RCP 8.5)

e

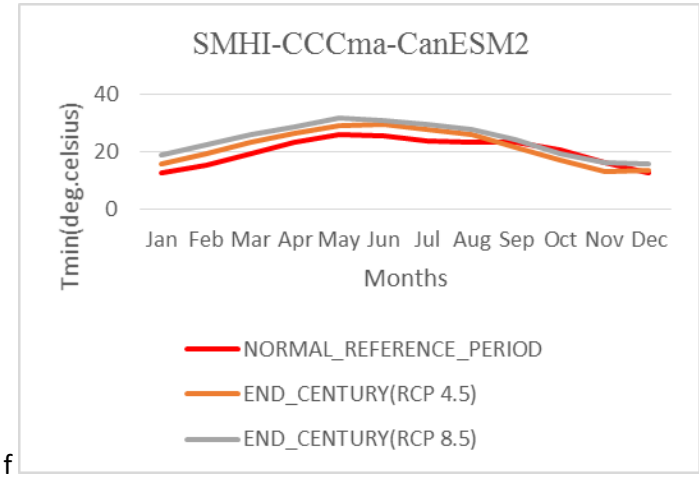
SMHI-CCCma-CanESM2
Tmin(deg.celsius)
40
20
0
Jan Feb Mar Apr May Jun Jul Aug Sep Oct Nov Dec
Months
NORMAL_REFERENCE_PERIOD
END_CENTURY(RCP 4.5)
END_CENTURY(RCP 8.5)

f

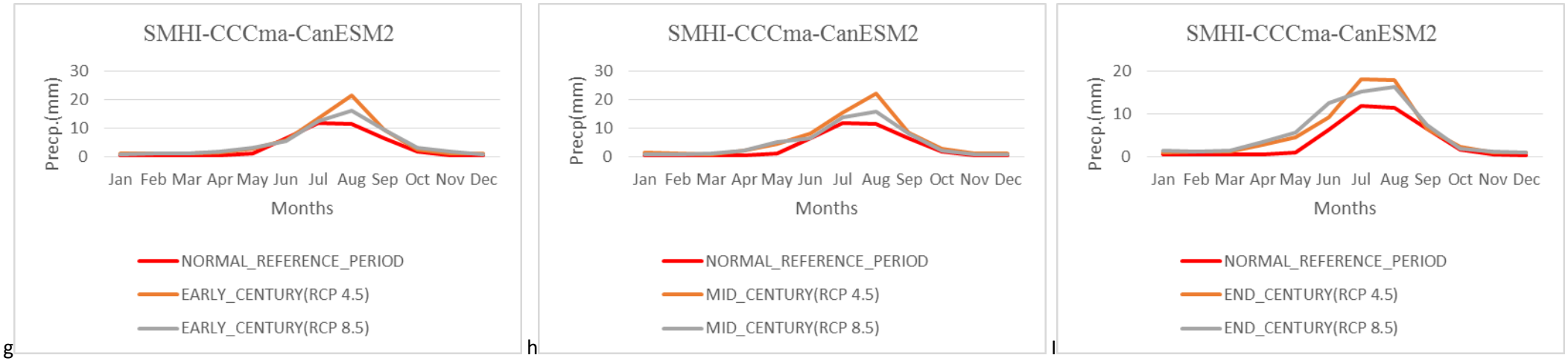

Figure 5. 9 (a-c) Tmax, (d-f) Tmin, (g-I) Pr average monthly comparison of future of SMHI-CCCma-CanESM2 for all three centuries under future projected RCP 4.5 and RCP 8.5 scenarios against reference periods.

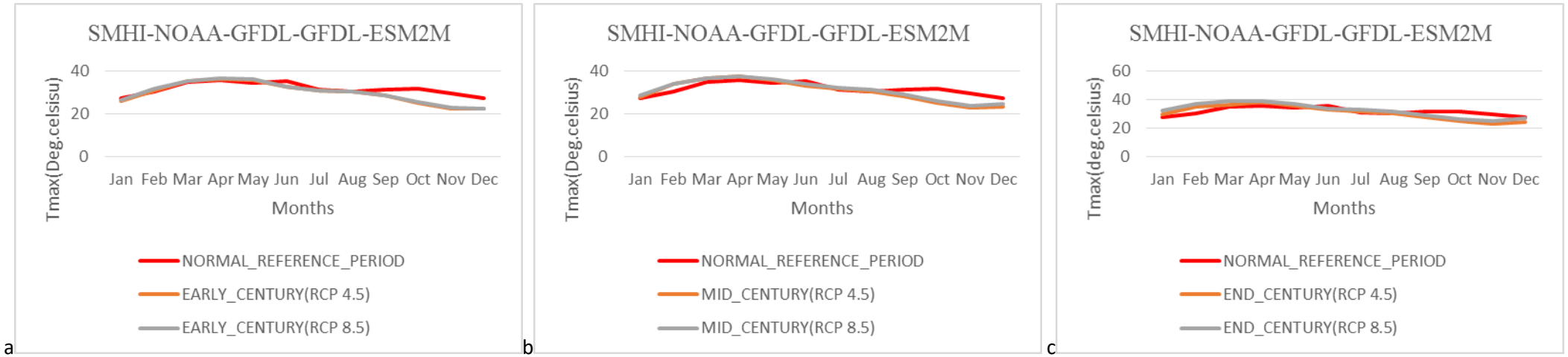

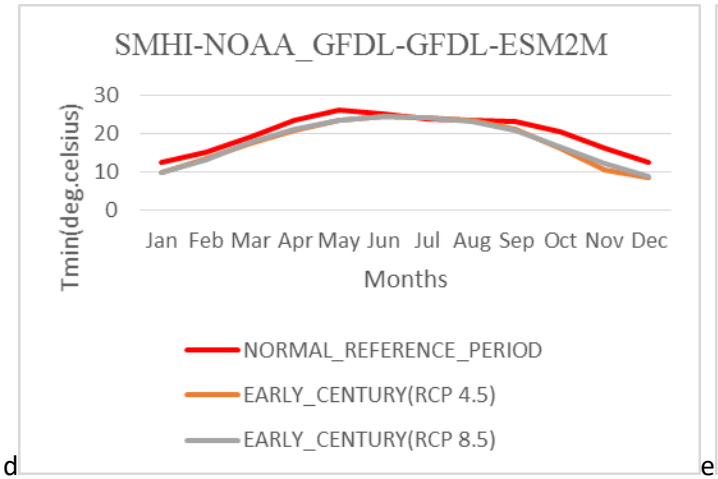

d

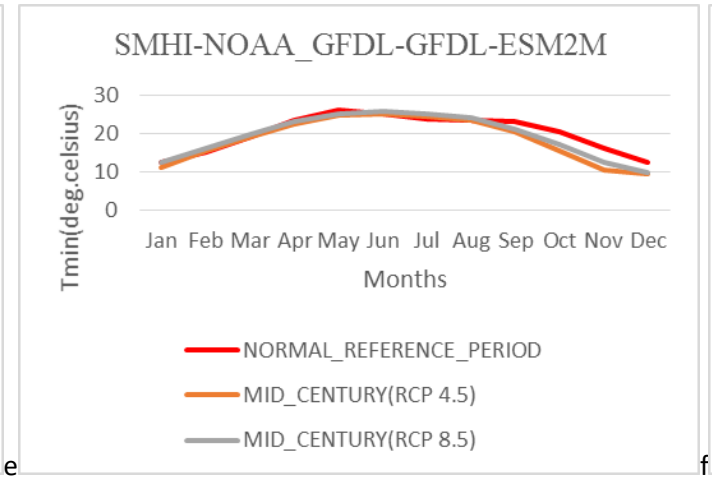

e

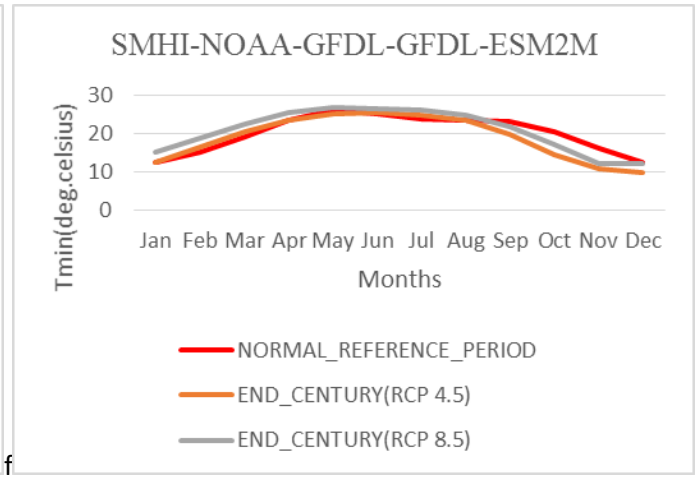

f

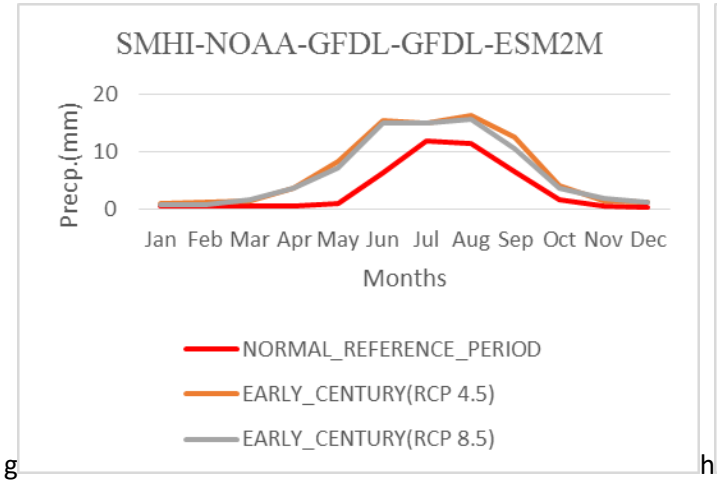

g

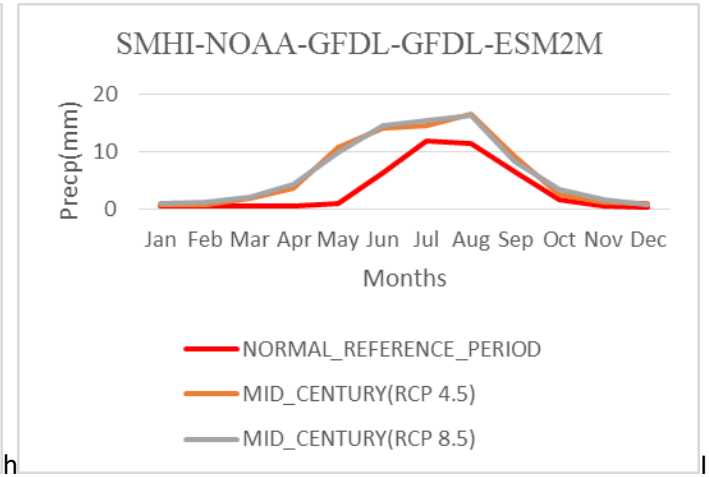

h

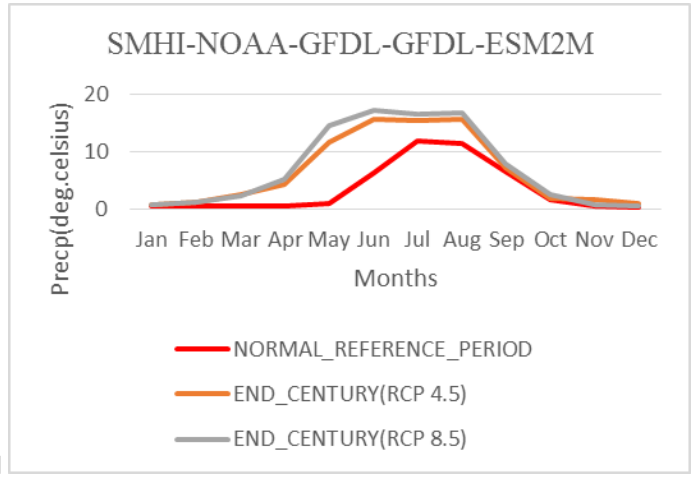

I

Figure 5. 10 (a-c) Tmax, (d-f) Tmin, (g-f) Pr average monthly comparison of SMHI-NOAA-GFDL-GFDL-ESM2M for all three centuries under future projected RCP 4.5 and RCP 8.5 scenarios against reference periods

Table 5. 2 Percentage change in Tmax, Tmin, Precipitation shown by IITM-CCCma-CanESM2 under the future climate change scenarios for RCP 4.5 and RCP 8.5.

IITM-CCCma-CanESM2	Early Century(2010-2039)	Mid Century(2040-2069)	End Century(2070-2099)
Percentage Change in Tmax	-5.5	-2.77	-2.13
Percentage Change in Tmin	4.35	9.08	10.64
Percentage change in precipitation	27.37	17.45	17.02
IITM-CCCma-CanESM2	Early Century(2010-2039)	Mid Century(2040-2069)	End Century(2070-2099)
Percentage Change in Tmax	-4.37	-1.58	2.11
Percentage Change in Tmin	6.21	11.67	19.32
Percentage change in precipitation	22.62	19.13	30.25

Table 5. 3 Percentage change in Tmax. Tmin, Precipitation shown by IITM-NOAA-GFDL-GFDL-ESM2M under the future climate change scenarios for RCP 4.5 and RCP 8.5.

IITM-NOOA-GFDL-GFDL-ESM2M	Early Century(2010-2039)	Mid Century(2040-2069)	End Century(2070-2099)
Percentage Change in Tmax	-7.57	-5.63	-5.23
Percentage Change in Tmin	-3.73	-0.72	0.05
Percentage change in precipitation	-4.37	-10.63	-8.45
IITM- NOOA-GFDL-GFDL-ESM2M	Early Century(2010-2039)	Mid Century(2040-2069)	End Century(2070-2099)
Percentage Change in Tmax	-7.43	-3.09	1.02
Percentage Change in Tmin	-3.40	3.40	10.14
Percentage change in precipitation	-3.84	-15.18	-17.92

Table 5. 4 Percentage change Tmax. Tmin, Precipitation shown by SMHI-CCCma-CanESM2 under the future climate change scenarios for RCP 4.5 and RCP 8.5.

SMHI-CCCma-CanESM2	Early Century(2010-2039)	Mid Century(2040-2069)	End Century(2070-2099)
Percentage Change in Tmax	7.35	9.53	11.15
Percentage Change in Tmin	0.94	5.67	8.48
Percentage change in precipitation	50.63	66.65	61.08
SMHI-CCCma-CanESM2	Early Century(2010-2039)	Mid Century(2040-2069)	End Century(2070-2099)
Percentage Change in Tmax	7.27	12.03	15.62
Percentage Change in Tmin	1.67	10.33	20.13
Percentage change in precipitation	36.22	39.30	65.56

Table 5. 5 Percentage change in Tmax, Tmin, precipitation shown by SMHI-NOAA-GFDL-GFDL-ESM2M under future climate change scenarios for RCP 4.5 and RCP 8.5.

SMHI-NOAA-GFDL-GFDL-ESM2M	Early Century(2010-2039)	Mid Century(2040-2069)	End Century(2070-2099)
Percentage Change in Tmax	-5.81	-3.46	-2.62
Percentage Change in Tmin	-11.65	-8.07	-6.22
Percentage change in precipitation	96.80	86.72	91.07
SMHI-NOAA-GFDL-GFDL-ESM2M	Early Century(2010-2039)	Mid Century(2040-2069)	End Century(2070-2099)
Percentage Change in Tmax	-5.22	-1.33	2.53
Percentage Change in Tmin	-10.59	-4.02	3.13
Percentage change in precipitation	85.01	90.92	108.27

5.4 Impact of Climate Change on Future River Discharge

5.4.1 Simulation of Historical Discharge

A comparison of river discharge for overlapping periods of IMD and CORDEX has been carried out to analyze the change in river discharge with reference to present. Average monthly observed discharge for the period of 1973-2004 as a reference data has been used for climate change projection studies. VIC model perform well in historical river discharge forced by IMD and CORDEX models data. The results showed good simulation on using both forcing so for further analysis same long-term observed discharge has been used for RCP4.5 and RCP8.5 at all three different centuries. Historical discharge comparison for all climate models as shown in Figure 5.11.

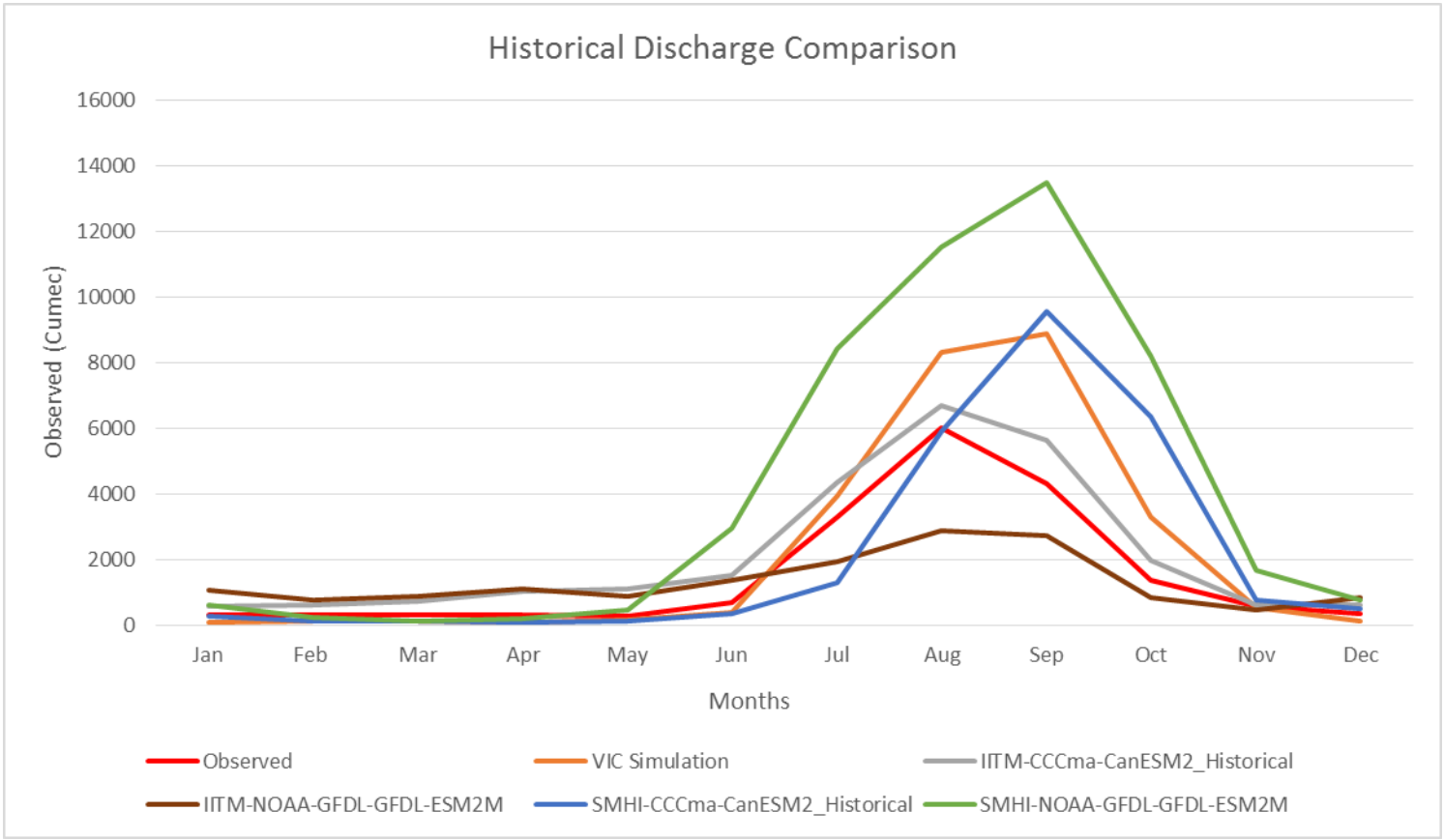

Figure 5. 11 Average monthly discharge comparison for (1973-2004) periods

Table 5. 6 Value obtain during historical simulation

Months	Observed	VIC Simulation	IITM-CCCma-CanESM2-Historical	IITM-NOAA-GFDL-GFDL-ESM2M-Historical	SMHI-CCCma-CanESM2-Historical	SMHI-NOAA-GFDL-GFDL-ESM2M-Historical
Jan	314.007	83.255	579.847	1051.252	265.010	630.093
Feb	307.622	131.722	600.589	768.573	140.108	251.614
Mar	302.762	107.987	726.956	879.771	135.836	133.139
Apr	303.620	92.058	1015.130	1119.302	86.502	202.172
May	274.702	154.873	1110.926	895.871	107.920	476.194
Jun	669.649	390.869	1511.882	1353.763	357.595	2939.925
Jul	3302.189	3939.943	4331.791	1947.561	1309.428	8411.885
Aug	6017.094	8298.759	6696.171	2880.292	5882.134	11512.804
Sep	4307.825	8892.050	5616.121	2720.001	9544.332	13484.032
Oct	1367.463	3310.193	1958.524	845.367	6340.908	8207.821
Nov	565.371	545.004	620.285	459.517	782.188	1680.105
Dec	336.433	110.251	622.923	838.498	510.314	758.732
Change Prediction	**1505.728**	**2171.414**	**2115.929**	**1313.314**	**2121.856**	**4057.376**

5.4.2 Future Projection on Simulated Runoff over the Basin

As observed from the sensitive analysis of future predicted, large change in surface runoff are projected for Mahanadi basin under the future climate in both RCP scenarios. The IITM-CAAma-CanESM2 is show that surface runoff is projected to increase in majority of Mahanadi Basin in End century (2070-2099) periods under both RCP 4.5 and 8.5 scenarios (Figure 5.12 (c)). The projected surface runoff is higher due to large increase in monsoon precipitation 10.64% in RCP 4.5 and 19.32% increase in RCP 8.5(Figure (I)). Significant variation was observed in early century (Figure (5.12(a)). Basin surface runoff is projected to increase significantly in RCP 4.5 and RCP 8.5 when compared with Midcentury.

On other side, IITM-NOAA-GFDL-GFDL-ESM2M climate model show large uncertainty in simulated surface runoff. It shows surface runoff is projected to decline in all estimated period under future climate scenarios. The decline in surface runoff may be due to less precipitation were predicted by the model (Figure 5.8(g, h, I)).

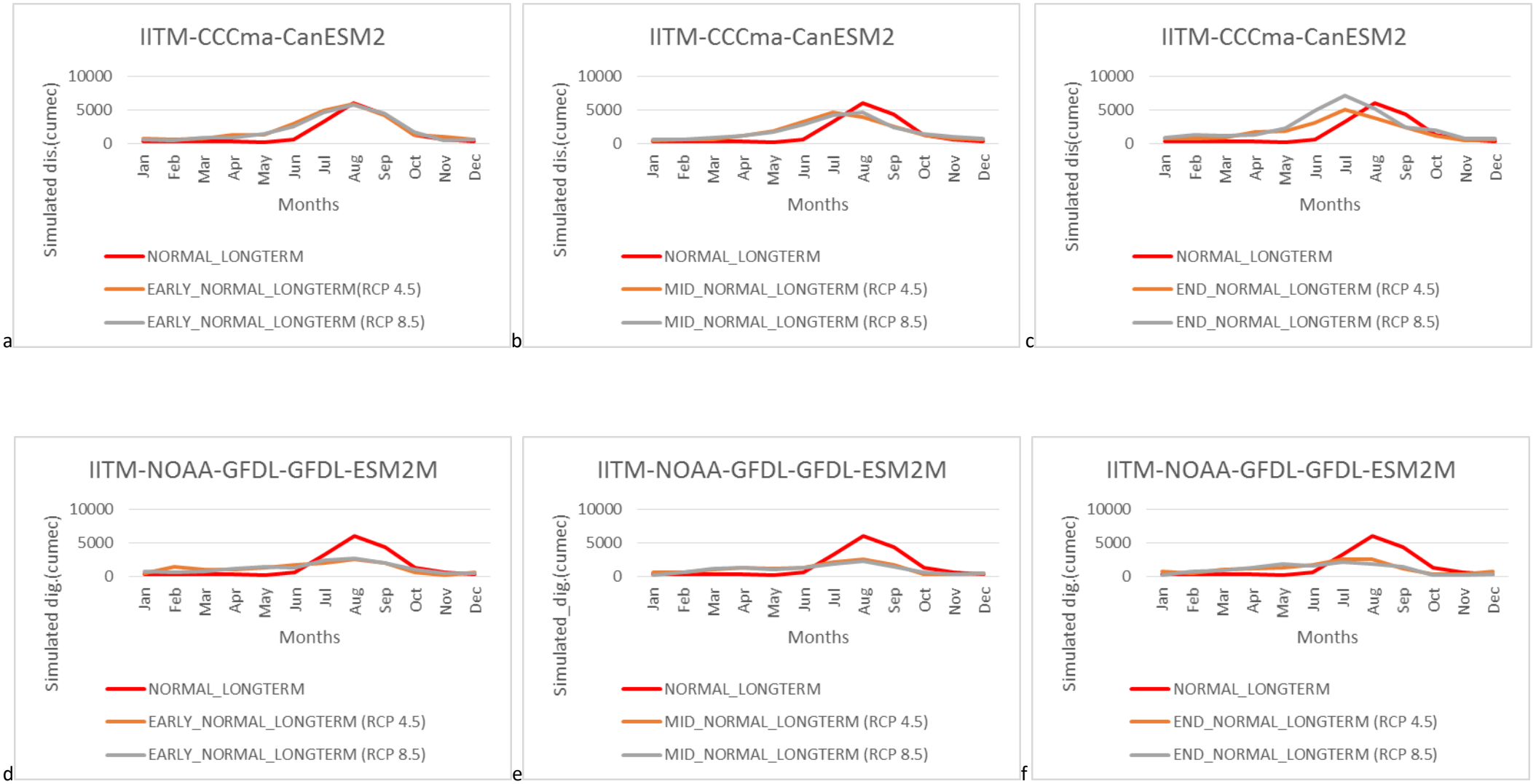

Figure 5. 12 (a-c) IITM-CCCma-CanESM2 & (d-f) IITM-NOAA-GFDL-GFDL-ESM2M projected simulated discharge comparison between RCP 4.5 and RCP 8.5 for all centuries.

SMHI climate model shows simulated projected future runoff differently under the future climate scenarios for RCP 4.5 and RCP 8.5. The results show that SMHI-CCCma-CanESM2 and SMHI-NOAA-GFDL-GFDL-ESM2M were simulated future surface runoff differently. Here peak runoff shifted toward September with high projected runoff compared from Normal Long-term (1973-2004) period. SMHI-CCCma-CanESM2 show uncertainty in RCP 4.5 where simulated runoff increased by 85.78% in Mid-century with respect to the reference period. It is even more than Mid-century for RCP 8.5 (Table 5.7). High surface runoff was estimated in End century where it increased by 105.07% (Table 5.7) under future climate scenario RCP 8.5. This change is mainly due to increase in precipitation as shown in Figure 5.4 and monsoon peak shift toward in August with high magnitude of simulated discharge (Figure 5.13(c)).

SMHI-NOAA-GFDL-GFDL-ESM2M show large change in simulated surface runoff under the future climate scenarios RCP 4.5 and RCP 8.5. Results show that in the end normal long-term period surface runoff increased due to received high precipitation (Table 5.5) and it increased by 214.65% in RCP 8.5 and 170.98% in RCP 4.5(Table 5.7), respectively.

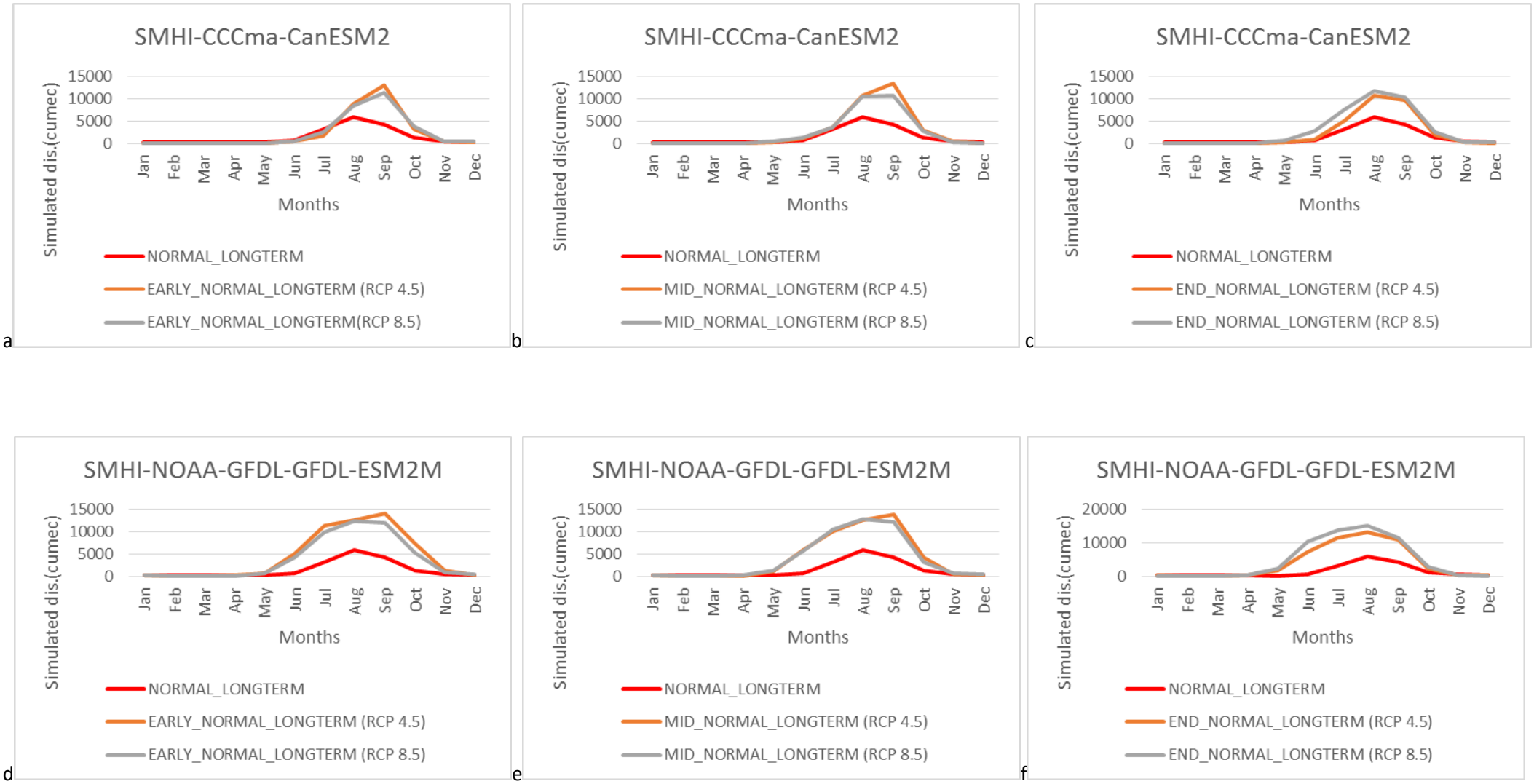

Figure 5. 13 (a-c) SMHI-CCCma-CanESM2 & (d-f) SMHI-NOAA-GFDL-GFDL-ESM2M projected simulated discharge comparison between RCP 4.5 and RCP 8.5 for all centuries

Table 5. 7 Percentage change in surface runoff under the future climate scenarios RCP 4.5 and RCP 8.5.

IITM-CCCma-CanESM2	Early Century(2010-2039)	Mid Century(2040-2069)	End Century(2070-2099)
RCP (4.5)	43.68	22.65	27.06
RCP(8.5)	37.25	25.82	67.004
IITM-NOAA-GFDL-GFD ESM2M	Early Century(2010-2039)	Mid Century(2040-2069)	End Century(2070-2099)
RCP(4.5)	-15.44	-24.17	-20.36
RCP(8.5)	-13.65	-29.51	-28.40
SMHI-CCCma-CanESM2	Early Century(2010-2039)	Mid Century(2040-2069)	End Century(2070-2099)
RCP(4.5)	59.66	85.78	64.48
RCP(8.5)	57.24	67.22	105.07
SMHI-NOAA-GFDL-GFD ESM2M	Early Century(2010-2039)	Mid Century(2040-2069)	End Century(2070-2099)
RCP(4.5)	195.42	172.83	170.98
RCP(8.5)	157.98	164.85	214.05

CHAPTER - 6

SUMMARY AND CONCLUSIONS

Distributed hydrological displaying offers a proficient answer for assess the long haul hydrological changes by permitting measurement of changes in stream designs.VIC hydrological model was used for Normal long-term discharge simulation. The VIC model showed a satisfactory performance when compared to observed discharge data during calibration and validation.

For climate change impact assessment, climate forcing which is driven from the output of four different climate models was used as input of meteorological forcing for calibrated hydrological models. Comparison of future projected river discharge was done on the basis average mean estimation. The outcomes got from the investigation demonstrated those surface overflows are touchier to the adjustment in precipitation and surface temperature. In addition, it was discovered that the adjustment in surface spillover and stream are to a great extent driven by the adjustment in precipitation instead of air temperature.

Execution of the variable infiltration capacity macro scale hydrological model to simulate stream flows during calibration and validation can be condensed as takes after.

a) Calibration simulation was done for the period 1990-1995 by comparing observed and simulated stream flow. The coefficient of determination during calibration was found to be 0.80.
b) The stream flow was found sensitive to upper layer parameter and bottom layer parameter. After changing these parameters, the model simulated better with high performance and the coefficient of determination as 0.81 at selected outlet (Tikapara).
c) Validation was done on the basis of calibrated parameter value for period (1996-2011) and simulation was found satisfactory with coefficient of determination as 0.77 at Tikapara.

In view of these perceptions, it can be inferred that model performance is good for hydrological simulation for Mahanadi basin. The calibrated and validated model was then used for future projection of river discharge under climate scenarios RCP 4.5 and RCP 8.5.

To analysis the climate change impact, changes in temperature and precipitation were investigate based on three 30-years period i.e. Early Century (2010-2039), Mid-Century (2040-2069), and End Century (2070-2099) in which Normal long-term (1974-2004) was taken as a reference period. The result showed that each climate models showed variability in the projected climate. IITM-CCCma-ESM2 showed increasing trend in precipitation and minimum temperature for estimated periods but surface max-temperature declined in both RCP 4.5 and RCP 8.5 climate scenarios when compared to the reference period. High consistency was observed between the two GCMs under single RCMs in terms of annual precipitation for the two GHGs emission scenarios. Under RCP 4.5 and RCP 8.5, large change in annual precipitation predicted by SMHI-NOAA-GFDL-GFDL-ESM2M on comparison with SMHI-CCCma-CanESM2. However, the increasing trend was predicted by SMHI-CCCma-CanESM2 in terms of surface temperature under RCP4.5 and RCP 8.5 respectively.

For future river discharge simulation, data of two RCMs at daily time step has been used which are respectively produced by IITM and SMHI. VIC hydrological model was calibrated for historical period and then runoff scenarios were generated by VIC calibrated model forced by four different CORDEX model climate data. Discrepancies were found in future discharge simulation. Simulation was based on three different centuries e.g. (Early Century (2010-2039), Mid Century (2040-2069), End Century (2070-2099) with Normal long-term (1973-2004) taken as a reference period. Result unmistakably demonstrates those streams are ending up more factors all through the basin. There are significant contrasts in the outcome between the atmosphere models e.g. SMHI-CCCma-CanESM2 and SMHI-NOAA-GFDL-GFDL-ESM2M show high projection in river discharge on compare with IITM- CCCma-CanESM2 and IITM- NOAA-GFDL-GFDL-ESM2M (Table 5.5) respectively.

Therefore, there will be large variability in the water availability in the catchment under future climate scenarios. So the decision or policy makers have to take or draw polices on water use accordingly. It is to be noted that there are large uncertainty in each model output. Therefore future work should be to assess these uncertainties.

REFERENCES

Bajracharya, A. R., Bajracharya, S. R., Shrestha, A. B., & Maharjan, S. B. (2018). Climate change impact assessment on the hydrological regime of the Kaligandaki Basin, Nepal. *Science of The Total Environment, 625*, 837-848.

Chen H, Chong YX, Shenglian G. (2012). Comparison and evaluation of multiple GCMs, statistical downscaling and hydrological models in the study of climate change impacts on runoff‖, Journal of Hydrology, 434–435 (2012) 36–4.

Dadhwal VK, Aggarwal S P and Misra N, (2010). Hydrological simulation of Mahanadi River basin and impact of landuse/ landcover change on surface runoff using a macro scale hydrological model, In International Society for Photogrammetry and Remote Sensing (ISPRS) TC VII Symposium – 100 years ISPRS, Vienna, Austria, 5–7 July 2010, ISPRS, vol. XXXVIII, Part 7B, pp. 165–170.

Garg, V., Khwanchanok, A., Gupta, P.K., Aggarwal, S.P., Kiriwongwattana, K., Thakur, P.K., &Nikam, B.R. (2012). Urbanization Effect on Hydrological Response: A Case Study of Asan River Watershed, India. Journal of Environment and Earth Science (IISTE), 2(9), 39-50

Garg V., Aggarwal, S.P., Gupta, P.K., Nikam, B.R., Thakur, P.K., Srivastav, S.K., &Senthil Kumar, A. (2017). Assessment of land use land cover change impact on hydrological regime of a basin. Accepted in Environmental Earth Sciences.

Garg, V., Nikam, B. R., Thakur, P. K., & Aggarwal, S. P. (2013). Assessment of the effect of slope on runoff potential of a watershed using NRCS-CN method. *International Journal of Hydrology Science and Technology*, *3*(2), 141-159.

Giorgi, F., C. Jones, and G. R. Asrar (2009), Addressing climate information needs at the regional level: the CORDEX framework, Bull. – World Meteorol. Organ, 58(3), 175 – 183.

IPCC (2013), Climate Change 2013: The Physical Science Basis. Contribution of Working Group I to the Fifth Assessment Report of the Intergovernmental Panel on Climate Change, Cambridge, UK.

IPCC (2000), Special report on emission scenarios, edited by N. Nakicenovic and R. Swart, Cambridge University Press, Cambridge, UK.

IPCC (2007), Climate change 2007: Synthesis Report. Contribution of Working Groups I, II and III to the Fourth Assessment Report of the Intergovernmental Panel on Climate Change, edited by R. K. Pachauri and A. Reisinger, Geneva, Switzerland.

J. Sanjay, M.V.S. Ramarao, M. Mujumdar, *et al.*Regional climate change scenarios M.N. Rajeevan, Shailesh Nayak (Eds.), Chapter of Book: Observed Climate Variability and Change over the Indian Region, Springer Geology (2017), pp. 285-304, 10.1007/978-981-10-2531-0

Kumar, N., Tischbein, B., Kusche, J., Laux, P., Beg, M. K., & Bogardi, J. J. (2017). Impact of climate change on water resources of upper Kharun catchment in Chhattisgarh, India. *Journal of Hydrology: Regional Studies*, *13*, 189-207.

Liang, X., Xie, Z., Huang, M.: A new parameterization for surface and groundwater interactions and its impact on water budgets with the variable infiltration capacity (VIC) land surface model. J. Geophys. Res. 108, 8-1–8-17 (2003)

Liang, X., Lattenmaier, D.P., Wood, E.F. and Burgess, S.J., 1994. A simple hydrologically based model of land surface, water, and energy flux for general circulation models. Journal of Geophysical Research, 99(D7): 14,415-14,428.

Liang, X., Lettenmaier, D.P. and Wood, E.F., 1996. One-dimensional Statistical Dynamic Representation of Subgrid Spatial Variability of Precipitation in the Two-Layer Variable Infiltration Capacity Model. J. Geophys. Res., 101(D16): 21,403-21,422.

Liu, Y., Zhang, X., Xia, D., You, J., Rong, Y., Bakir, M.: Impacts of land-use and climate changes on hydrologic processes in the Qingyi River Watershed, China. J. Hydrol. Eng. 18, 1495–1512 (2013)

Lohmann, D., et al. (1996), a large scale horizontal routing model to be coupled to land surface parameterization schemes, Tellus (48A), 708-721.

Lohmann, D., et al. (1998a), Regional scale hydrology: I. Formulation of the VIC-2L model coupled to a routing model, Hydrol. Sci. J.-J. Sci. Hydrol., 43(1), 131-141.

Lohmann, D., et al. (1998b), Regional scale hydrology: II. Application of the VIC-2L model to the Weser River, Germany, Hydrol. Sci. J.-J. Sci. Hydrol., 43(1), 143-158.

Lohmann, D., et al. (2004), Streamflow and water balance Intercomparison of four land surface models in the North American Land Data Assimilation System project, J. Geophys. Res.-Atmos., 109(D7), 22.

Lutz, A. F., ter Maat, H. W., Biemans, H., Shrestha, A. B., Wester, P., & Immerzeel, W. W. (2016). Selecting representative climate models for climate change impact studies: an advanced envelope-based selection approach. *International Journal of Climatology*, *36*(12), 3988-4005.

Mishra, V., & Lilhare, R. (2016). Hydrologic sensitivity of Indian sub-continental river basins to climate change. *Global and Planetary Change*, *139*, 78-96.

Mishra, V., Keith, A.C., Dev, N., Ming, L., Bryan, C.P., Deepak, K.R., Bowling, L., Guoxiang, Y.: A regional scale assessment of land use/land cover and climatic changes on water and energy cycle in the upper Midwest United States. Int. J. Climatol. 30, 2025–2044 (2010)

Moss, R. H. et al. (2010), The next generation of scenarios for climate change research and assessment., Nature, 463(7282), 747 – 56, doi:10.1038/nature08823.

Meehl, G. A., C. Covey, T. Delworth, M. Latif, B. Mcavaney, J. F. B. Mitchell, R. J. Stouffer, and K. E. Taylor (2007), The WCRP CMIP3 multimodel dataset: A New Era in Climate Change Research, Bull. Am. Meteorol. Soc., 88(September), 1382 – 1394.

Maurer, E. P., et al. (2001), Evaluation of the land surface water budget in NCEP/NCAR and NCEP/DOE reanalyzes using an off-line hydrologic model, J. Geophys. Res.-Atmos., 106(D16), 17841-17862.

Nijssen, B., et al. (1997), Streamflow simulation for continental-scale river basins, Water Resour Res, 33(4), 711-724.

Nijssen, B., et al. (2001a), Predicting the discharge of global rivers, J. Clim., 14(15), 3307-3323.

Nijssen, B., et al. (2001b), Global retrospective estimation of soil moisture using the variable infiltration capacity land surface model, 1980-93, J. Clim., 14(8), 1790-1808.

Nijssen, B., et al. (2003), Simulation of high latitude hydrological processes in the Torne-Kalix basin: PILPS phase 2(e) - 2: Comparison of model results with observations, Global Planet Change, 38(1-2), 31-53.

Qiao, L., Hong, Y., Renee, M.R., Mark, S., David, G.D., David, W.D., Chen, S., Lilly, D.: Climate Change and Hydrological Response in the Trans-State Oologah Lake Watershed-Evaluating Dynamically Downscaled NARCCAP and Statistically Downscaled CMIP3 Simulations with VIC Model BCSD. Water Resour. Manag. 28, 3291–3305 (2014)

Suoquan Zhou, Xu Liang, Jing Chen & Peng Gong (2014) An assessment of the VIC-3L hydrological model for the Yangtze River basin based on remote sensing: a case study of the Baohe River basin, Canadian Journal of Remote Sensing, 30:5, 840-853, DOI: 10.5589/m04-031

Sanjay, J., Krishnan, R., Shrestha, A. B., Rajbhandari, R., & Ren, G. Y. (2017). Downscaled climate change projections for the Hindu Kush Himalayan region using CORDEX South Asia regional climate models. *Advances in Climate Change Research*, *8*(3), 185-198.

Tan, M. L., Yusop, Z., Chua, V. P., & Chan, N. W. (2017). Climate change impacts under CMIP5 RCP scenarios on water resources of the Kelantan River Basin, Malaysia. *Atmospheric Research*, *189*, 1-10.

Taylor, K. E., R. J. Stouffer, and G. A. Meehl (2012), An Overview of CMIP5 and the Experiment Design, Bull. Am. Meteorol. Soc., 93(4), 485 – 498, doi:10.1175/BAMS-D-11-00094.1.

Van Vuuren, D. P. et al. (2011b), the representative concentration pathways: an overview, Climate. Change, 109(1-2), 5 – 31, doi: 10.1007/s10584-011-0148-z.

Yan, D., Werners, S. E., Ludwig, F., & Huang, H. Q. (2015). Hydrological response to climate change: The Pearl River, China under different RCP scenarios. *Journal of Hydrology: Regional Studies*, *4*, 228-245.

Appendix-1

The surface of each grid in the cell can contain multiple LULC classes and/or vegetation tiles. This is represented in Figure 2. The surface is mathematically described as n=N+1 land cover tiles, where N=1, 2, 3…..N. N represents different land cover tiles and n represents the bare soil. For each vegetation tile, the vegetation characteristics, such as LAI, albedo, minimum stomatal resistance, architectural resistance, roughness length, relative fraction of roots in each soil layer, and displacement length (in the case of LAI) are assigned and then land cover (vegetation) classes are specified (Fig 2).

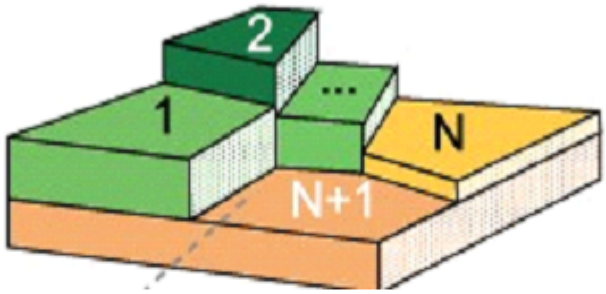

Figure 2. 1 Grid cell vegetation coverage

Source:
http://www.hydro.washington.edu/Lettenmaier/Models/VIC

Associated with each land cover type are a single canopy layer, and multiple soil layers. In this study, for example, two different soil layers have been used, the first extending to a depth of 0.3 meters and the second extending to a depth of 0.5 meters. The canopy layer intercepts rainfall according to a Biosphere-atmosphere transfer scheme (BATS) parameterization (Dickinson, et al. 1986) as a function of LAI. All information about the vegetation is input through vegetation library and vegetation parameter file (Blondin 1991) (Docuudre 1993). Within a grid cell infiltration, moisture flux between the runoff and soil layers are calculated according to the vegetation cover type. Surface runoff and base flow are calculated separately considering each vegetation type and then summed over the composition vegetation within each grid cell (Franchini and M. 1991).

2. Soil layers

Soil characteristics can be signified for a user defined number of vertical layers usually two or three, dividing into thin upper layer and secondary set of layers. Soil parameters for each grid and soil layer is specified in user defined soil parameter file (Zhao 1980). Different soil texture classifications exist in literature, including the USDA classification and the NBSSLUP classification of soil. In the current study, soil texture classes have been determined using the NBSSLUP classification and the parameters for different soil properties have been estimated according the USDA classification given in the VIC Manual.

3. Rainfall

The rainfall that a grid cell receives is distributed throughout all or a portion of a grid cell. This is a function of rainfall intensity and aligns with the use of sub-grid variability that the VIC model considers. The equation used to distribute precipitation is-

$$\mu = (1\text{-}e^{\text{-}aI})$$

Where,

I = Precipitation intensity

a = coefficient which describes the effect of grid cell size and geography

The fractional coverage of precipitation over a grid cell changes with the intensity of precipitation of a storm ie. It increases with increase in storm precipitation intensity and vice versa. The Soil water content in every grid cell is set to average before the occurrence of a storm.

4. Evapotranspiration

Evapotranspiration is calculated according to the Penman-Monteith equation, in which the evapotranspiration is a function of net radiation and vapor pressure deficit. Total actual evapotranspiration is the sum of canopy evaporation and transpiration from each vegetation tile and bare soil evaporation from the bare soil tile, weighted by the coverage fraction for each surface cover class. The VIC model take into account three different types of evaporation: evaporation from the canopy layer (Ec, mm) of each vegetation class, transpiration (Et, mm) from each vegetation class and evaporation from the bare soil (E1, mm). Total evapotranspiration over a grid cell is calculated as the sum of the above components, weighted by the respective surface cover area fractions (Liang, et al. 1996).

The equation is expressed as-

$$\lambda_v E_p = \frac{\Delta (R_n - G) + \rho_a c_p (e_s - e_p) / r_a}{\Delta + \gamma}$$

Where,

λ_v = latent heat of vaporation (J kg^{-1})

R_n = net radiation (W m^{-2})

G = soil heat flux (W m^{-2})

$e_s - e_a$ = vapor pressure deficit of the air (Pa)

ρ_a = density of air at constant pressure (kg m^{-3})

c_p = Specific heat of the air (J kg^{-1} K^{-1})

Δ = slope of the saturation vapor pressure temperature relationship (Pa K^{-1})

γ = psychrometric constant (66 Pa K^{-1})

5. Infiltration

Infiltration is the process by which the water made available at the surface of soil, enters the soil (Philip 1957). . This model assumes that infiltration capacity of the soil is not uniform. According to topography, soil and vegetation, the runoff generation and evaporation will vary. The model considers infiltration storage and not rate. That is, it comes up with a volumetric value for infiltration for a given period of time. Since VIC considers sub-grid variability, this is applied while calculating the infiltration capacity of a particular grid. To represent variable infiltration capacity as a function of relative saturated area of the grid cell, this uses a spatial probability distribution (Liang, et al. 1994) (Liang, et al. 1996).

The equation used to model infiltration capacity is based on the formula used in Xinanjang model which assume that precipitation in excess of the available infiltration capacity forms surface runoff. The equation is-

$$i = i_m(1 - (1 - A)^{\frac{1}{b_i}})$$

Where,

i = Infiltration capacity up to which the soil is filled

i_m = Maximum infiltration capacity

A = represents the saturated fraction of the grid cell (0=A=1)

b_i = shape parameter

The amount of soil moisture plays an important role in the infiltration capacity; this parameter is calculated with the following equation-

$$W_{c1} = \frac{i_m}{1 + b_i}$$

6. Base flow

Baseflow is the delayed flow that reaches the stream essentially as groundwater flow (Subramanya 2008). There is no direct way to continuously measure base flow throughout a basin or processes that affect base flow such as overland flow, evapotranspiration, interflow, and groundwater recharge (Furey and Gupta 2001). Thus, VIC is often used to calculate the baseflow through calibration. Baseflow is a function of hydraulic conductivity of the soil, as well as the drainage between two different soil layers. In the VIC model, baseflow is derived as the function of soil moisture in the lowest soil layer using Arno-nonlinear formula.

$$Q_b = \frac{D_s D_m}{W_s W_{c2}} W_2^- \quad 0 \le W_2^- W_s W_{c2}$$

$$Q_b = \frac{D_s D_m}{W_s W_{c2}} W_2^- + \left(1 - \frac{D_s}{W_s}\right) D_m \left(\frac{W_2^- - W_s W_{c2}}{W_{c2} - W_s W_{c2}}\right)^2 \quad \text{for} \quad W_2^- \ge W_s W_{c2}$$

Where,

D_m = Maximum base flow parameter

D_s = Fraction of Maximum base flow

W_s = Fraction of maximum soil moisture

W_{c2} = Maximum soil moisture in layer 2

W_2^- = soil moisture content at the beginning of time step in layer 2

6. Routing

In the VIC model, every grid cell is sculptured severally while not horizontal water flow. The grid-based VIC model simulates the statistics of runoff just for every grid cell that is non-uniformly distributed among the cell. So that, a complete routing model (Lohmann, et al., 1996) (Lohmann, et al., 1998) is utilized to moved grid cell surface runoff and base flow to the outlet of that grid cell then into the stream system. Within the routing model, water isn't allowed to result the channel in to the grid cell. Once it reaches the channel, it's now not a part of the water budget. Figure 6 shows the schematic of the routing model.

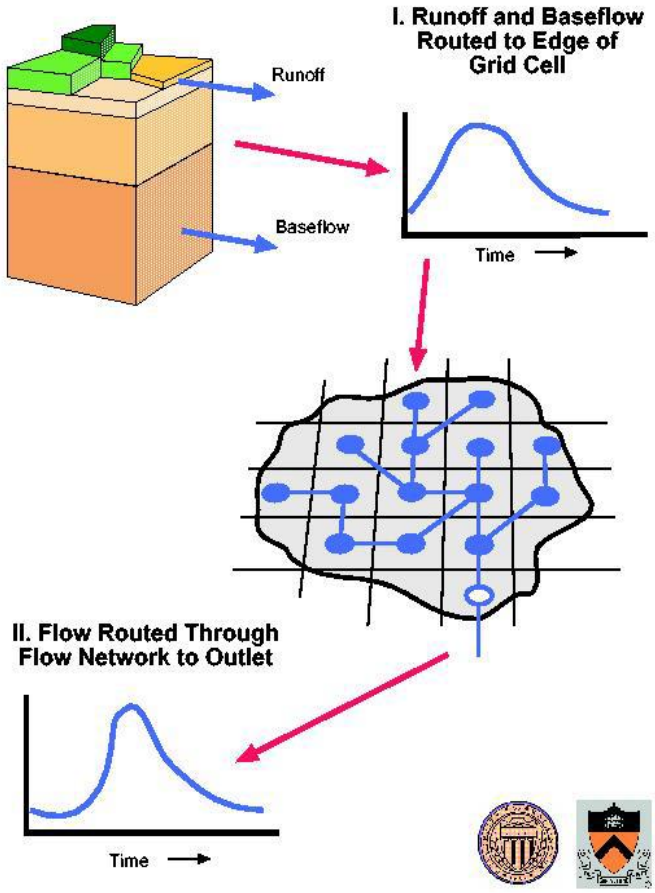

Figure 2. 1 Schematic of VIC network routing models

Routing is employed to predict the outflow hydrograph of watersheds subjected to a notable quantity of precipitation. Routing model related to VIC principally consists of inside grid cell routing and routing between cells. Inside grid routing element considers the time needed for creating runoff inside a grid cell to reach an arbitrary outlet. The runoff generated by VIC model for every grid cell is convolved with a separate unit hydrograph,

$$R_1 = \sum_{j=1}^{i<j} Q_j H_{i\ j-1}$$

Where,

R_1 = internally routed runoff at the grid cell outlet

Q_j = Run off outflow at Vic

I = Time step of unit hydrograph

j = Time step of runoff time series

i = Total number of time steps in runoff

H = Unit hydrograph ordinates

While routing between cells, the internally routed runoff R_1 is transported downstream through the flow network after lagging with an effective velocity of 1 ms^{-1}. The effective velocity is near the lower end of the range suggested by Susen. The inclusion of the stream routing model (Fig 6), developed by (Lohmann, et al., 1998) permits comparisons between the model-derived discharge and observations at gauging stations.

7. Various Modes of VIC Model

7.1 Water Balance

Water balance mode assumes that land surface temperature equals air temperature. This mode does not solve the full surface energy balance, exception is the snow algorithm that still solves the surface energy balance to determine the fluxes required to drive accumulation and ablation procedures. This mode needs comparatively less time for computation than other modes due to removal of the ground heat flux solution and iterative procedure required to close the surface energy balance. The time step range from hourly to daily.

The daily water balance mode is significantly faster than sub-daily simulations. Parameters needed for daily water balance simulation are different from those which used for sub-daily simulation. The daily water balance model can be used to simulate discharge from a river basin, parameters for the daily water balance model are not transfer to any model which run with a sub-daily time step. While running this model in water balance mode we need to define at least three parameters such as rainfall, maximum and minimum temperature at daily time scale.

7.2 Energy Balance

Full energy balance mode calculates all water and energy fluxes close to land surface, and run time step could also be one or three hours. The surface energy balance is closed by a repetitious procedure that tries to seek out a surface temperature that adjusts surface energy fluxes (ground heat, sensible heat, ground heat storage, outgoing radio radiation and indirect latent heat). Hence this mode need a lot of procedure time than water balance in addition as needs sub-

daily simulation time step. Finally this mode simulates the surface energy fluxes, which are important to understand the hydrologic cycle and land surface-atmosphere interactions in a basin. While running this model in full energy balance mode we need to define rainfall, maximum & minimum temperature and wind speed at sub-daily scale.

7.3 Frozen Soil

Frozen soil affects both moisture and energy fluxes. It solves thermal fluxes at nodes through the soil column using the finite difference method as well as it computes the maximum unfrozen water content at each soil node based on the nodal temperature. Also ice content for each soil moisture layer is calculated from the nodal values and is used to restrict infiltration and soil moisture drainage. In addition to that the nodal ice contents are also used to derive the soil thermal conductivity and volumetric heat capacity for the next model time step.

7.4 Special case

Optimization of output, model state and debug code modes are special cases which can be applied to both energy balance and water balance to get output as desired by the user. They modify output in the described fashion and can be controlled by pre-processor commands in user deft which needs to be set before the source code is compiled.

Appendix -2

Overview of Vegetation library file

Variable Name	Units	Number of Values	Description
veg class	N/A	1	Vegetation class identification number (reference index for library table)
over story	N/A	1	Flag to indicate whether or not the current vegetation type has an overstory (TRUE for overstory present [e.g. trees], FALSE for overstory not present [e.g. grass])
rarc	s/m	1	Architectural resistance of vegetation type (~2 s/m)
rmin	s/m	1	Minimum stomatal resistance of vegetation type (~100 s/m)
LAI		12	Leaf-area index of vegetation type
albedo	fraction	12	Shortwave albedo for vegetation type
rough	M	12	Vegetation roughness length (typically 0.123 * vegetation height)
displacement	M	12	Vegetation displacement height (typically 0.67 * vegetation height)
wind_h	M	1	Height at which wind speed is measured.
RGL	W/m^2	1	Minimum incoming shortwave radiation at which there will be transpiration. For trees this is about 30 W/m^2, for crops about 100 W/m^2.
rad_atten	fract	1	Radiation attenuation factor. Normally set to 0.5, though may need to be adjusted for high latitudes.
wind_atten	fract	1	Wind speed attenuation through the overstory. The default value has been 0.5.
trunk_ratio	fract	1	Ratio of total tree height that is trunk (no branches). The default value has been 0.2.
comment	N/A	1	Comment block for vegetation type. Model skips end of line so spaces are valid entrys.

(Source: http://www.hydro.washington.edu)

Appendix- 3

Overview of vegetation parameter files

Sl. no	Variable Name	Units	Description
1	Grid cell	N/A	Grid cell number
2	Vegetation type no	N/A	Number of vegetation types in a grid cell
3	Veg class	N/A	Vegetation class identification number
4	Cv	fraction	Fraction of grid cell covered by vegetation type
5	Root depth	m	Root zone thickness (sum of depths is total depth of root penetration)
6	Root fraction	fraction	Fraction of root in the current root zone

(Source: http://www.hydro.washington.edu)